ACS Infectious Diseases

Subscriber access provided by UNIV OF NEW ENGLAND ARMIDALE

Article

Development of biphenylthiazoles exhibiting improved pharmacokinetics and potent activity against intracellular Staphylococcus aureus

Mohamed Hagras, Nader S. Abutaleb, Noha Elhosseiny, Tamer M. Abdelghany, Mariam Omara, Mohamed Elsebaei, Marwa Alhashimi, Allison B Norvil, Mark I Gutay, Humaira Gowher, Ahmed Attia, Mohamed N. Seleem, and Abdelrahman S Mayhoub

ACS Infect. Dis., **Just Accepted Manuscript** • DOI: 10.1021/acsinfecdis.0c00137 • Publication Date (Web): 08 Sep 2020

Downloaded from pubs.acs.org on September 10, 2020

Just Accepted

"Just Accepted" manuscripts have been peer-reviewed and accepted for publication. They are posted online prior to technical editing, formatting for publication and author proofing. The American Chemical Society provides "Just Accepted" as a service to the research community to expedite the dissemination of scientific material as soon as possible after acceptance. "Just Accepted" manuscripts appear in full in PDF format accompanied by an HTML abstract. "Just Accepted" manuscripts have been fully peer reviewed, but should not be considered the official version of record. They are citable by the Digital Object Identifier (DOI®). "Just Accepted" is an optional service offered to authors. Therefore, the "Just Accepted" Web site may not include all articles that will be published in the journal. After a manuscript is technically edited and formatted, it will be removed from the "Just Accepted" Web site and published as an ASAP article. Note that technical editing may introduce minor changes to the manuscript text and/or graphics which could affect content, and all legal disclaimers and ethical guidelines that apply to the journal pertain. ACS cannot be held responsible for errors or consequences arising from the use of information contained in these "Just Accepted" manuscripts.

is published by the American Chemical Society. 1155 Sixteenth Street N.W., Washington, DC 20036

Published by American Chemical Society. Copyright © American Chemical Society. However, no copyright claim is made to original U.S. Government works, or works produced by employees of any Commonwealth realm Crown government in the course of their duties.

Development of biphenylthiazoles exhibiting improved pharmacokinetics and potent activity against intracellular *Staphylococcus aureus*

Mohamed Hagras[1‖], Nader S. Abutaleb[2‖], Noha M. Elhosseiny,[3] Tamer M. Abdelghany,[4] Mariam Omara,[4] Mohamed M. Elsebaei[1], Marwa Alhashimi[2], Allison B Norvil[5], Mark I Gutay[5], Humaira Gowher[5,6], Ahmed S. Attia,[3] Mohamed N. Seleem[2,7*] and Abdelrahman S. Mayhoub[1,8*]

[1] Department of Pharmaceutical Organic Chemistry, College of Pharmacy, Al-Azhar University, 1-Elmokhayem Eldaem Street, Cairo 11884, Egypt.

[2] Department of Comparative Pathobiology, College of Veterinary Medicine, Purdue University, 725 Harrison Street, West Lafayette, IN 47907, USA.

[3] Department of Microbiology and Immunology, Faculty of Pharmacy, Cairo University, Cairo, Egypt, 11562.

[4] Department of Pharmacology and Toxicology, College of Pharmacy, Al-Azhar University, 1-Elmokhayem Eldaem Street, Cairo 11884, Egypt.

[5] Department of Biochemistry, College of Agriculture, Purdue University, West Lafayette, IN 47907, USA.

[6] Purdue University Center for Cancer Research, Purdue University, West Lafayette, IN 47907, USA

[7] Department of Biomedical Sciences and Pathobiology, Virginia-Maryland College of Veterinary Medicine, Virginia Polytechnic Institute and State University, Blacksburg, VA, 24061, USA.

[8] University of Science and Technology, Nanoscience Program, Zewail City of Science and Technology, Ahmed Zewail Street, October Gardens, 6th of October, Giza 12578, Egypt

Corresponding Authors. *e-mail: mseleem@purdue.edu, amayhoub@azhar.edu.eg

[‖]These two authors contributed equally

Exploring the structure-activity-relationship (SAR) at the cationic part of arylthiazole antibiotics revealed hydrazine as an active moiety. The main objective of the study is to overcome the inherited-toxicity associated with the free-hydrazine. A series of hydrocarbon bridges was inserted in between, to separate the two amino groups. Hence, the aminomethylpiperidine-containing analog **16** was identified as a new promising antibacterial agent with efficient antibacterial and pharmacokinetic profiles. Briefly, compound **16** outperformed vancomycin in terms of the antibacterial spectrum against vancomycin-resistant staphylococcal and enterococcal strains with minimum inhibitory concentrations (MICs) ranging from 2 to 4 μg/mL, faster bactericidal mode of action, completely eradicating the high staphylococcal burden within 6-8 hours, and a unique ability to completely clear intracellular staphylococci. In addition, the initial pharmacokinetic assessment confirmed the high metabolic stability of compound **16** (biological half-life > 4 h), good extra-vascular distribution and maintaining a plasma concentration higher than the average MIC value for over 12 h. Moreover, compound **16** significantly reduced MRSA burden in an *in vivo* MRSA skin infection mouse experiment. These attributes collectively suggest compound **16** as a good therapeutic candidate for invasive staphylococcal and enterococcal infections. From a mechanistic point of view, compound **16** inhibited undecaprenyl diphosphate phosphatase (UppP) with an IC_{50} value of 29 μM.

Keywords: antibiotic resistance, methicillin-resistant *Staphylococcus aureus*, vancomycin-resistant enterococci, intracellular infections, pharmacokinetics.

According to the World Health Organization (WHO) global priority list of antibiotic-resistant bacteria, Methicillin-resistant, vancomycin-intermediate and vancomycin-resistant *Staphylococcus aureus* (MRSA, VISA and VRSA) are categorized as high priority for which new antibiotics are urgently needed.[1] Although applying strong preventive measures in hospitals over the last fifteen years alleviated the rapid spread of hospital-acquired MRSA infections, this progress did not last for a long time. In 2017, reductions of hospital-acquired MRSA infections stalled and the community-acquired MRSA increased, causing around 20,000 deaths in the USA alone as per the Centers for Disease Control and Prevention (CDC).[2] The majority of the current antibiotics used to treat MRSA infections are associated with some limitations and toxic side effects. For instance, vancomycin is not recommended for patients with reduced kidney function such as the elderly or diabetic patients.[3] Additionally, linezolid toxicity is associated with 26% mortality where some patients develop lactic acidosis, myelosuppression, optic or peripheral neuropathies, and myopathies.[4-5] Furthermore, several incidences of *S. aureus* strains resistant to the currently used antibiotics such as vancomycin, linezolid, and daptomycin have been documented.[3, 6, 7] Consequently, the rising MRSA resistance to the commonly used antibiotics, along with the increased infection cases (both hospital- and community-acquired) highlight the critical need for new entities to treat MRSA infections.

Despite the first wave of staphylococcal resistance that was mediated by the secretion of penicillinase,[8] current multidrug-resistant staphylococci developed different mechanisms to sustain the fight against modern antibacterial agents. One mechanism utilized by the bacteria is its ability to invade the host phagocytes to avoid the human immune system.[9] Staphylococci developed several mechanisms to suppress the phagocytic lysosomal enzymes, and to survive at low pH inside macrophages.[10] Different multidrug-resistant *Staphylococcus aureus* strains release

staphylococcal-borne toxins such as LukAB, which suppress the protective function of macrophages.[11] Moreover, they can compensate for the harsh cytosolic environment by the slowing down their growth rate to adapt to the intracellular media. Consequently, the ability of *S. aureus* to deceive the immune system and pretend to be a cell component resulted in increasing the resistance burden.[12] to further exacerbate the problem, around 40% of patients with MRSA-induced pneumonia experience a life-threatening slow response to vancomycin, the drug of choice for systemic staphylococcal infections.[13] Therefore, finding a new antibacterial agent with the ability to resolve the problematic intracellular MRSA is an urgent medical need.

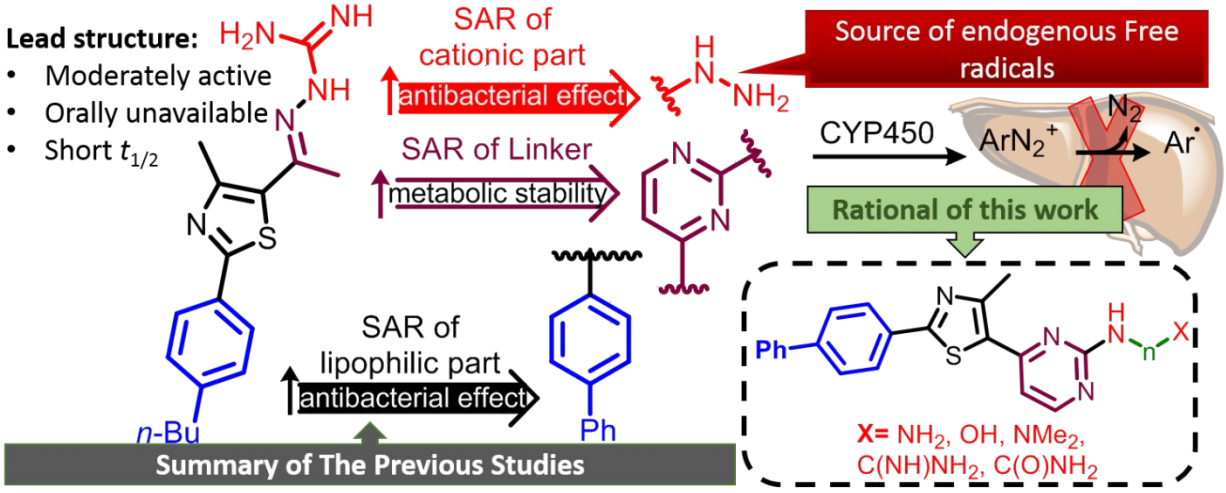

Figure 1. Progress in phenylthiazole project and aim of the current work.

One of our successfully discovered new antibacterial scaffolds is arylthiazole that demonstrated confirmed activity against a large panel of multidrug-resistant (MDR)-Gram positive pathogens.[14-24] These compounds outperformed vancomycin in terms of their rapid bactericidal mode of action.[25-26] The structure-activity relationships (SAR) of arylthiazole antibacterial core were studied from three different perspectives. Briefly, the biphenyl side chain revealed notable improvement in the antibacterial effect,[27] while the short half-life of the first discovered lead compound was remarkably enhanced by inserting the C=N linker within pyrimidine structure

(Figure 1).[28] Lastly, intensive efforts were reported to optimize the cationic part, in which the hydrazine moiety potentiates the antibacterial activity (Figure 1).[28] Hydrazine and hydrazine-like structures are considered toxicophores that increase the incidence of oxidative stress in living tissues.[29-30] Hence, hydrazine moiety is an uncommon structural motif in approved therapeutics, and those containing such toxic moiety, isoniazid as an example, are associated with black box-warning due to acute hepatotoxicity.[31] Hydrazine-containing structures exert their toxic effect via metabolic activation into diazonium derivative and subsequent generation of aryl free radicals.[32] As a strategy to overcome this problem, the two amino groups of hydrazine motif were separated by a short hydrocarbon chain (Figure 1). Hence, it is chemically or metabolically impossible to generate a diazonium intermediate. The antibacterial activity of all newly synthesized compounds were investigated, and the pharmacokinetic behavior of the most promising derivative was studied as well.

RESULTS AND DISCUSSION

CHEMISTRY. The synthetic route started with the reaction between bisphenylthioamide **1** and α-chloroacetylacetone, which afforded bisphenylthiazole **3**. The later was allowed to react dimethylformamide-dimethylacetal to yield the intermediate **4**, which then subjected to react with thiourea, and the product was methylated with dimethyl sulfate to give the methylmercaptopyrimidine derivative **5**. Oxidation of **5** with a per-acid provided the key intermediate **6**, which used to obtain the final products **7-25** (Scheme 1).

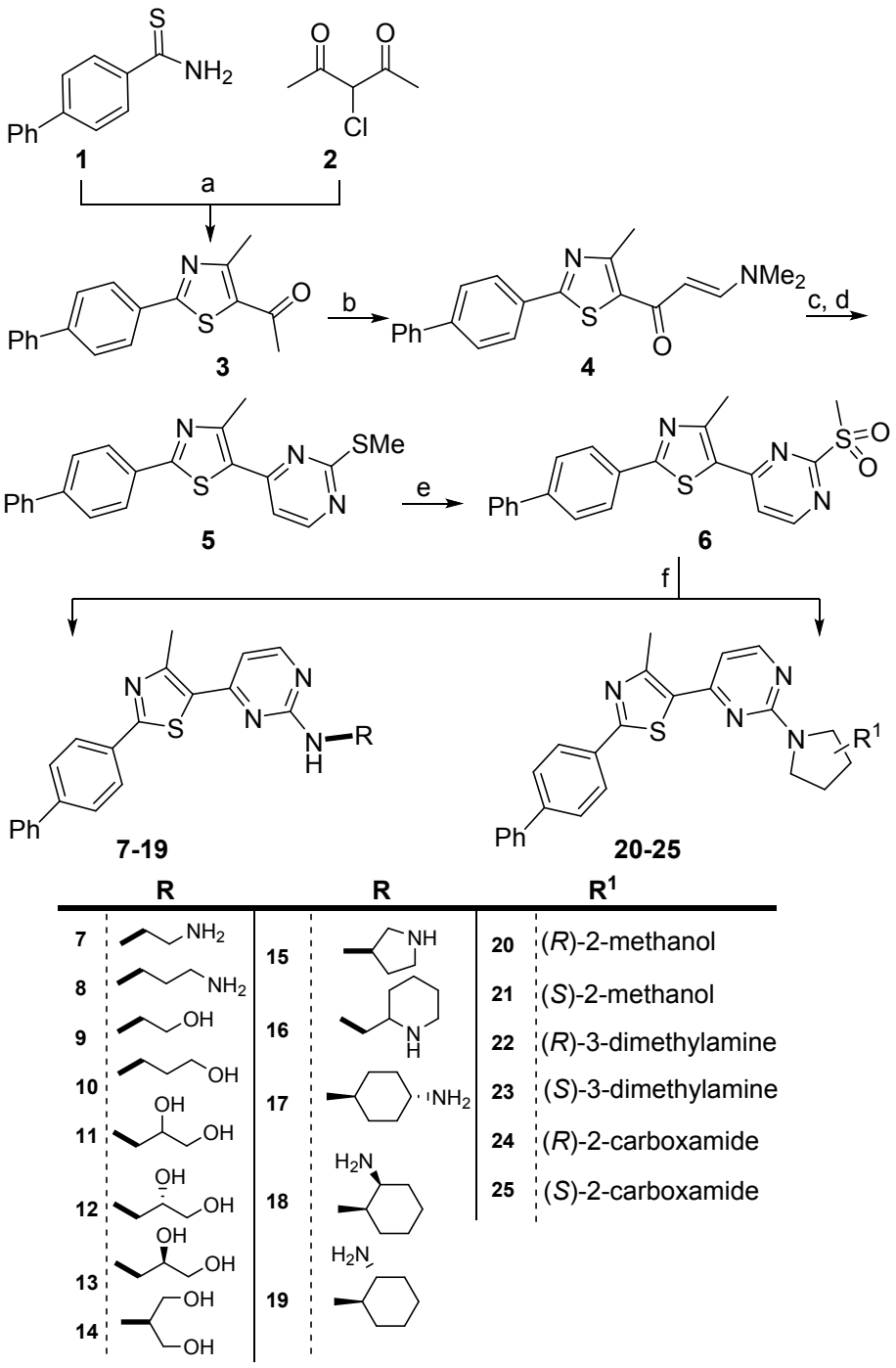

Reagents and conditions: (a) Absolute EtOH, 3-chloropentane-2,4-dione, heat at reflux, 12 h; (b) DMF-DMA heat at 80 °C, 8h; (c) thiourea, KOH, EtOH, heat at reflux, 8 h; (d) dimethyl sulfate, KOH, H_2O, stirring at 23 ^oC, 2 h; (e) MCPBA, dry DCM, stirring at 23 ^oC, 16 h; (f) appropriate amine, dry DMF, heat at 80 ^oC for 0.5 - 8h.

Scheme 1. Synthetic pathway of compounds **7-25**

BIOLOGICAL RESULTS AND DISCUSSIONS. As mentioned earlier, the main purpose of this study was to find a bioisostere for the toxicophore hydrazine moiety. Since hydrazine is not an intrinsic toxic group by itself and it needs hepatic activation to generate the corresponding toxic diazonium intermediate, we decided to first add small alkyl chain between its two amino groups. Obviously, this chemical modification prevents the formation of diazonium intermediate and consequently the toxic free radicals. The ethylenediamine and propylenediamine derivatives **7** and **8** were synthesized and tested for their antimicrobial activities. Both compounds were moderately active against MRSA USA300 with MIC value of 16 μg/mL (Table 1). The next set of structural modifications included conformationally-restricted analogs **15**-**19**. First, by incorporating the terminal nitrogen within an alicyclic ring system, a divergence in antibacterial activity was observed. While the pyrrolidinyl derivative **15** was void from any antibacterial activity, the piperidinyl analog **16** exhibited high potency against MRSA with an MIC value of 2 μg/mL (two-fold higher than the frontline therapeutic vancomycin) (Table 1). Second, restricting the free rotation of ethylene bridge by loading both amino groups on a cyclic structure gave compounds **18** and **19**, in which the geometric relationships of the two amino groups was investigated. In this vein, both compounds were 2 to 4 times more potent than the ethylenediamine-containing derivative **7** while the trans-isomer **19** possessed two-fold better anti-MRSA activity than its cis-form **18**. On the other hand, the nullified activity of the trans-1,4-diamine derivative **17** highlights the crucial importance of the shorter two to three-carbons linker.

All attempts to functionalize the terminal amine by methylation, replacement with hydroxyl isostere or incorporating within an amide structure ended up with inactive compounds

with the exception of the (*S*)-dimethylaminopyrrolidine **23** that revealed moderate activity against MRSA with an MIC value of 8 μg/mL.

Table 1. Initial antibacterial assessment, MIC values in μg/mL

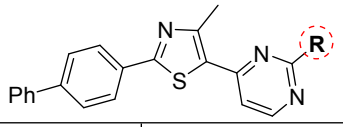		**NRS384 (MRSA USA300)**
7	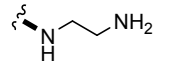	16
8	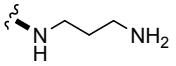	16
15	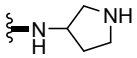	>64
16	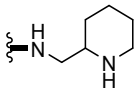	2
18	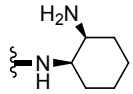	8
19	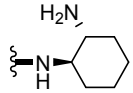	4
17	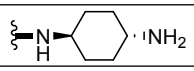	>64
24	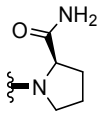	>64
25	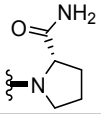	>64
23	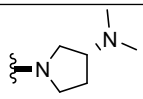	8
22	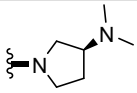	32
9	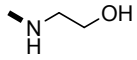	>64
10	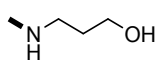	>64
14	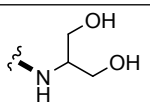	>64
12	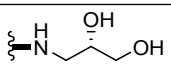	>64

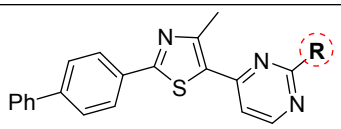		**NRS384 (MRSA USA300)**
11	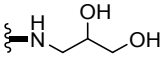	>64
13	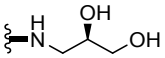	>64
21	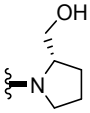	>64
20	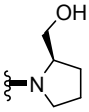	>64
vancomycin	N/A	1

For the promising new antibacterial compounds **16** and **19**, several attributes need to be investigated such as studying the activity against a large panel of MDR-bacteria that belong to different genera, high selectivity to the prokaryotic cells over mammalian cells, mode of killing and killing kinetics, the likelihood of developing resistance to it, and the ability to target intracellular pathogens. Therefore, in the next sections, we will present a comprehensive microbiological profile of the most potent derivatives (compounds **16** and **19**).

The promising antibacterial activity of compounds **16** and **19** was further confirmed against a panel of clinically relevant MDR-staphylococcal strains including linezolid-resistant and vancomycin-resistant *S. aureus* strains and methicillin-resistant *Staphylococcus epidermidis*. The compounds maintained their level of inhibition against all the tested *S. aureus* isolates (MIC = 2-4 μg/mL), and compound **16** was superior to **19** MIC value of 2 μg/mL against most of the tested strains (Table 2). They also, exhibited potent activity against *S. epidermidis*, a common colonizer of the human skin, and a common source of implanted medical prosthetic devices infections. *S. epidermidis* infections are tough to be treated due to their huge ability to form strongly adherent biofilms that have intrinsic resistance to antibiotics and the host defense systems.[33-34] Moreover,

both compounds exhibited bactericidal activity against the tested strains where their MBC values were the same as or one-fold higher than their corresponding MICs.

Table 2. MICs and MBCs (μg/mL) of compounds **16** and **19** against staphylococcal clinical isolates.

Bacterial Strains	**Compounds**/control antibiotics							
	19		**16**		Linezolid		Vancomycin	
	MIC	**MBC**	**MIC**	**MBC**	**MIC**	**MBC**	**MIC**	**MBC**
MSSA ATCC 6538	4	4	2	2	1	16	1	2
MSSA NRS 107	2	2	4	4	0.5	64	1	2
MRSA NRS119	4	4	2	2	32	> 64	1	1
MRSA NRS123 (USA400)	4	4	2	4	1	16	1	2
MRSA NRS 385 (USA500)	4	8	2	2	0.5	32	1	2
MRSA NRS 386 (USA700)	4	8	2	2	1	64	0.5	1
VRSA 10	4	4	2	2	0.5	64	64	> 64
VRSA 12	4	4	2	4	1	32	64	> 64
Methicillin-resistant *Staphylococcus epidermidis* NRS101	2	4	2	2	0.5	16	0.5	1

MSSA, methicillin-sensitive *Staphylococcus aureus*; MRSA, methicillin-resistant *Staphylococcus aureus*; VRSA, vancomycin-resistant *Staphylococcus aureus*

In coincidence with the activity against *S. aureus* strains, compounds **16** and **19** exhibited potent antibacterial activity against other clinically important drug-resistant Gram-positive bacteria, inhibiting the growth of tested strains at concentrations ranging between 2 and 4 μg/mL (Table 3). The compounds maintained their activity against vancomycin-resistant enterococci (VRE) (Table 3), a leading cause of nosocomial infections in the USA that cause about 20%-30% of hospital-acquired infections and the second major cause of such infections across the world.[35] Additionally, compounds **16** and **19** exhibited potent activities against *Streptococcus pneumoniae*, with MICs ranging from 2-4 μg/mL. *S. pneumoniae* is the leading cause of bacterial pneumonia and meningitis in the USA and a major cause of bloodstream, ear and sinus infections. It is associated with more

than 2,000,000 infections annually in the USA, resulting in more than 6,000 deaths and an estimate of $4 billion total costs.[36] Moreover, in more than 30% of infections, the bacteria are resistant to one or more clinically relevant antibiotics.[36] Interestingly, the compounds' MBC values were the same as or one-fold higher than their corresponding MICs indicating that they exhibited bactericidal activity against the tested strains.

Table 3. MICs and MBCs (μg/mL) of compounds **16** and **19** against non-*Staphylococcus aureus* clinical isolates.

Bacterial Strains	**Compounds**/control antibiotics							
	19		**16**		Linezolid		Vancomycin	
	MIC	**MBC**	**MIC**	**MBC**	**MIC**	**MBC**	**MIC**	**MBC**
Vancomycin-resistant *Enterococcus faecalis* ATCC 51299	4	8	2	4	0.5	16	32	> 64
Vancomycin-resistant *Enterococcus faecium* ATCC 700221	4	8	2	4	1	32	>64	>64
***Listeria monocytogenes* ATCC 19111**	2	2	1	2	0.5	16	0.5	1
Cephalosporin-resistant *Streptococcus pneumoniae* ATCC 51916	4	4	4	8	1	32	1	1
Methicillin-resistant *Streptococcus pneumoniae* ATCC 700677	4	8	2	8	0.5	16	1	2

Next. in order to test confirm the bactericidal activity of the compounds, a time-killing assay was performed against MRSA USA400. Figure 2 indicates that compound **19** exhibited a rapid bactericidal activity by reducing more than 3-$\log_{10}$ CFU within only 2 hours and completely eradicated MRSA burden after 6 hours. On the other hand, compound **16** reduced the high MRSA inoculum by more than 3-$\log_{10}$-reduction after 6 hours and completely killed that high inoculum after 8 hours. In contrast, vancomycin, the drug of choice, eradicated the high MRSA count after 24-hours. This fast-bactericidal mode of action adds an additional clinical value to our newly

developed compounds as both drugs of choices, in such cases, (vancomycin and linezolid) possess their own drawbacks that affect the overall clinical efficacy. The former is a very slow-bactericidal agent,[37] while the latter has a bacteriostatic mode of action,[38] resulting in difficulty in clearing bacterial infections in many cases.[39-40]

Due to the rapid bacterial killing, it is thought that it is hard (or at least a slow rate) for a bacterium to develop resistance against an antibacterial agent with a rapid bactericidal mode of action.[41] As reported previously, the main target of phenylthiazoles is the inhibition of two consecutive proteins involved in bacterial cell wall biosynthesis.[26] This consecutive inhibition might explain the inability of MRSA to develop resistance against phenylthiazoles, as reported earlier.[17] To test whether the new compounds **16** and **19** are susceptible to the development of resistance by MRSA, a multi-step resistance test was conducted. Unlike rifampicin, to which MRSA developed resistance rapidly, the MIC values for compounds **19** and **16** increased by only one-fold after the eighth and fourteenth passage, respectively; but they remained stable thereafter (Figure 3). This result indicates that MRSA cells could not develop rapid resistance to phenylthiazole antibiotics which could provide this newly emerging class of antibiotics with an expected long-term clinical efficacy.

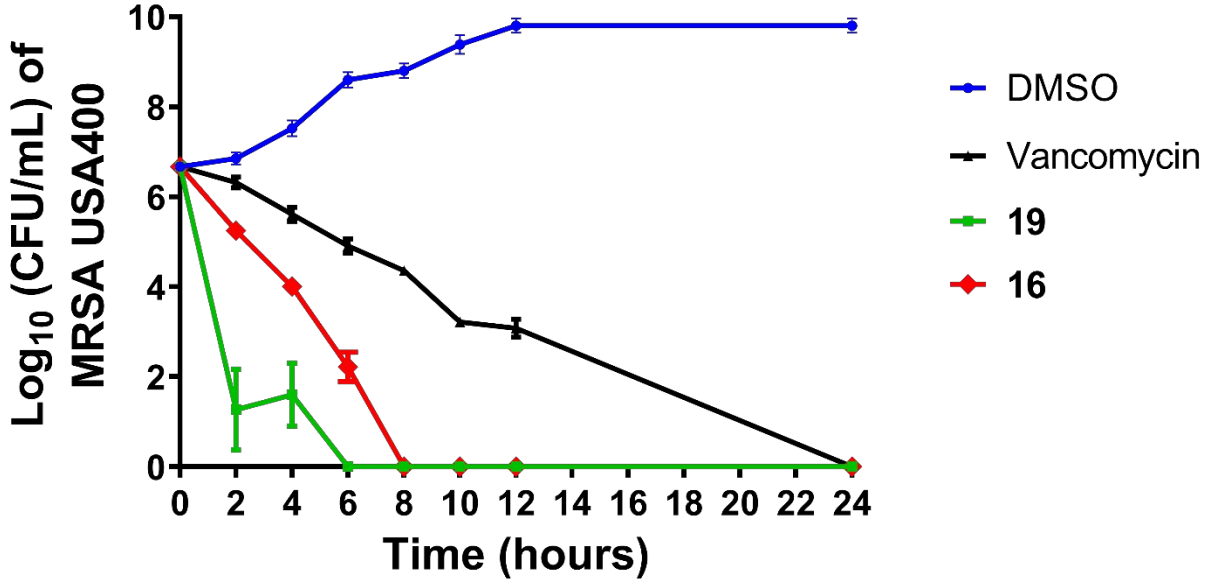

Figure 2. Killing kinetics of compounds **16** and **19** (tested in triplicates at 5 × MIC) against methicillin-resistant *Staphylococcus aureus* (MRSA USA 400) over a 24-hour incubation period at 37 ℃. DMSO (solvent for the compounds) served as a negative control and vancomycin served as a control drug. The error bars represent standard deviation values obtained from triplicate samples used for each compound/antibiotic studied.

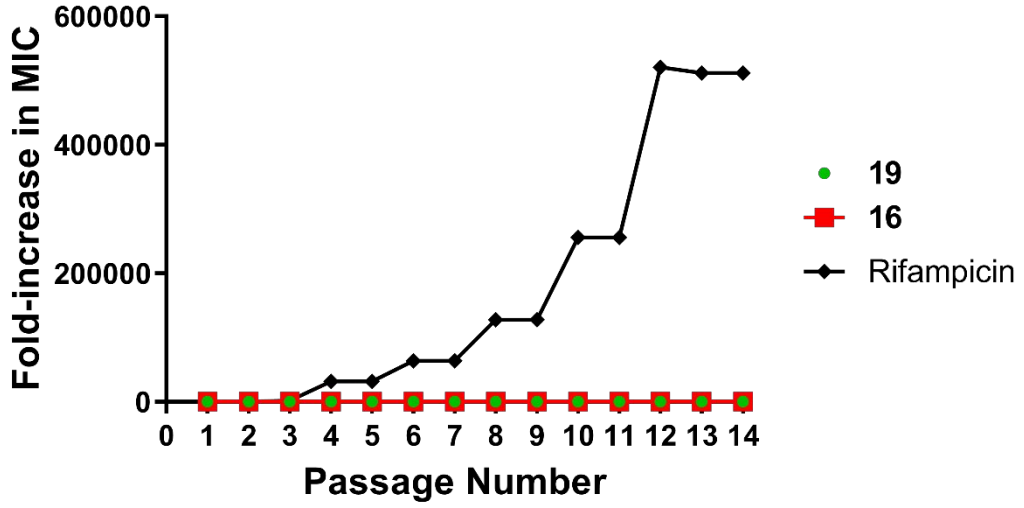

Figure 3. Multi-step resistance selection of compounds **16**, **19** and rifampicin against methicillin-resistant *S. aureus* USA400 (NRS123). Bacteria were serially passaged over a 14-day period and the broth microdilution assay was used to determine the MIC of each compound against MRSA after each successive passage. A four-fold shift in MIC would be indicative of bacterial resistance to the test agent.

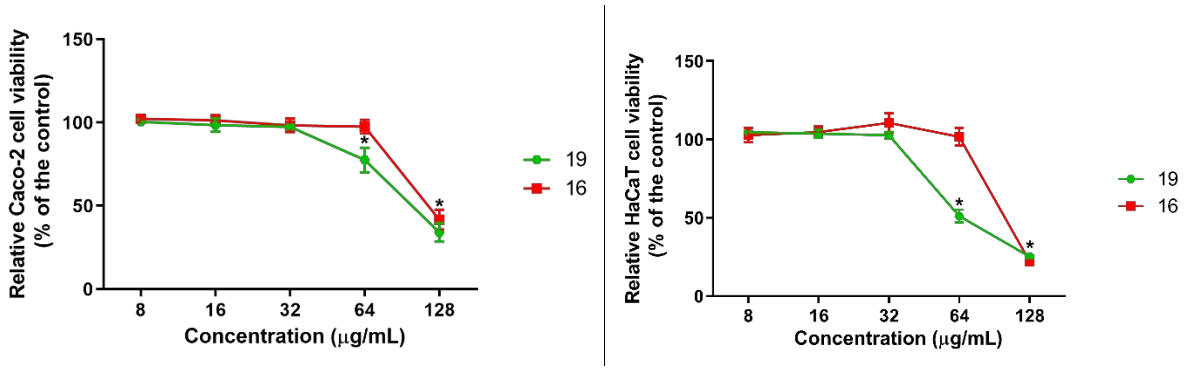

Figure 4. Analyzing the toxicity of compounds **16** and **19** (tested in triplicates at 8, 16, 32, 64 and 128 μg/mL) against human colorectal cells (Caco-2) (***Left***) & against human keratinocyte cells (HaCaT) (***Right***) using the MTS 3-(4,5-dimethylthiazol-2-yl)-5-(3-carboxymethoxyphenyl)-2-(4-sulfophenyl)-2*H*-tetrazolium) assay. Results are presented as percent viable cells relative to DMSO (negative control to determine a baseline measure for the cytotoxic impact of each compound). The absorbance values represent an average of three samples analyzed for each compound. Error bars represent standard deviation values. Data were analyzed via a two-way ANOVA with post hoc Dunnett's test for multiple comparisons. Asterisks (*) denote a statistically significant difference ($P<0.05$) between values obtained for the compounds as compared to the DMSO-treated samples.

After confirming the potent bactericidal activity against multiple MDR-bacterial strains, mode of killing kinetics and a low tendency of resistance development, we moved next to test compounds' tolerability by examining the cytotoxicity of compounds **16** and **19** against two mammalian cells, Caco-2 and HaCaT cells (Figure 4). Caco-2 cell line was used to get a preliminary insight about the tolerability of the compounds to the human colon cells if administered orally, and HaCaT cells were employed to investigate the toxicity of the compounds to human skin cells if applied topically. Both compounds exhibited a good toxicity profile on Caco-2 cells, where they exhibited well tolerability at high concentrations. Briefly, compound **16** was non-toxic to Caco-2 and HaCaT cells at a concentration as high as 64 μg/mL where about 100% of the cells were viable. This concentration represents 32-times its corresponding MIC values against MRSA strains. On the other hand, the diaminocyclohexyl derivative **19** was slightly less tolerable for both tested cell lines.

The last studied parameter in the bacteriological profiling is the ability of these compounds to keep their efficacy against intracellular pathogens. Most antibiotics including the drugs of choice for MRSA infections such as vancomycin and linezolid, exhibit limited activity against intracellular bacteria due to several reasons such as low levels of accumulation intracellularly, inactivation by the acidic pH within macrophages, or binding to lysosomal contents. To assess the intracellular killing ability of our newly synthesized phenylthiazole compounds, an infected murine macrophage (J774) model was used. By testing the tolerable concentration to murine macrophage cells, it was found that both tested compounds **16** and **19** were tolerable to J774 at a concentration up to 16 µg/mL, where almost 100% of the cells were viable (Figure S1). Therefore, at a non-toxic concentration (4× MIC), compound **16** had the highest intracellular clearing activity by completely eradicating the intracellular MRSA burden (below the limit of detection (10 CFU/mL)). On the other hand, compound **19** reduced the intracellular MRSA burden by 2.08-$\log_{10}$-reduction (about 99.18% reduction) at 4× MIC (16 µg/mL) (Figure 5).

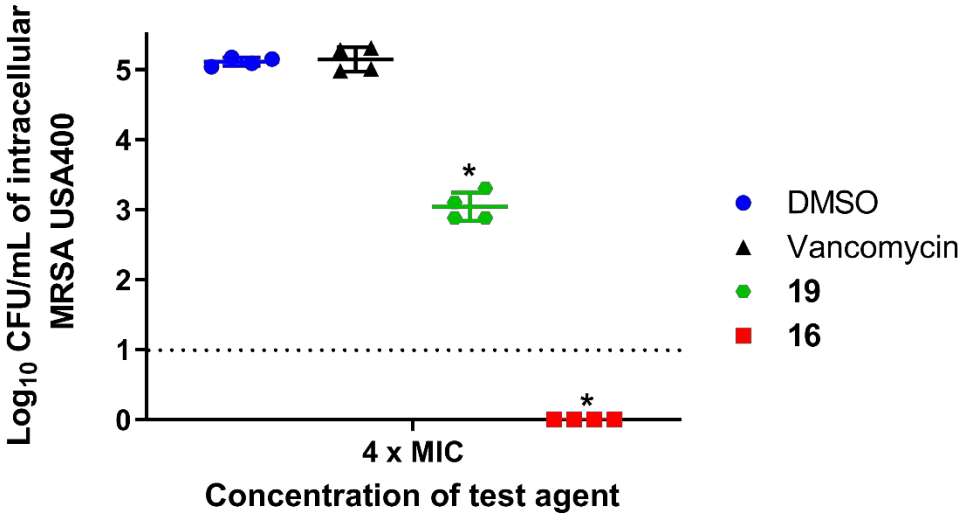

Figure 5. Examination of the activity of compounds **16** and **19** on the clearance of intracellular MRSA present in murine macrophage (J774) cells. Data are presented as $\log_{10}$ CFU/mL of intracellular MRSA USA400 inside infected murine macrophages after treatment with 4× MIC of

either compounds **16**, **19** or vancomycin (tested in quadruplicates) for 24 hours. Data were analyzed via one-way ANOVA, with post hoc Dunnet's test for multiple comparisons ($P < 0.05$), utilizing GraphPad Prism 6.0 (GraphPad Software, La Jolla, CA). Asterisks (*) denotes statistically significant difference between treatment with either compounds **16** or **19** compared to vancomycin.

So far, the microbiological screening and profiling boil down to suggest compound **16** as a promising novel antibacterial candidate. Therefore, the next section will focus on exploring the key pharmacokinetic parameters in order to decide, whether compound **16** can be further developed into a systemically administered antibiotic or its use will be limited to topical applications. In this vein, incubation of compound **16** with liver microsomes indicated a high level of metabolic stability with an intrinsic half-life ($intT_{1/2}$) value of more than 2.5 hours (Table 4). This value went down to around 1.5 hours when the same compound was incubated in absence of NADPH, the co-factor of CYP450, indicating that compound **16** is a substrate for other liver metabolic enzyme(s) rather than the CYP450. Furthermore, the *in vitro* metabolic stability of compound **16** was translated into a biological half-life ($t_{1/2}$) value of 4.3 h, after being administered as an intravenous (IV) bolus to rats (Figure 6). The pharmacokinetic curve after single IV dose revealed, in addition to highly acceptable $t_{1/2}$ value, a good distribution in biological tissues other than the vascular system, as indicated by the value of its volume of distribution in the 2nd compartment (Vβ).

Table 4. *In vitro* preliminary pharmacokinetic parameters; half-life and intrinsic clearance ($T_{1/2}$ and Cl_{int}) of compounds 16.

Compound	Incubation Time (min)	% Compound Remaining			Half-Life (min)			Cl_{int} (μL/min/mg)
		1st	2nd	Mean	1st	2nd	Mean	
16 (with NADPH)	0	100.0	100.0	100	162.9	145.8	154.4	44.9
	15	111.4	100.2	106				
	30	105.2	102.7	104				
	45	100.2	98.0	99				
	60	76.6	70.8	74				
16 (no NADPH)	0							

Compound	Incubation Time (min)	% Compound Remaining			Half-Life (min)			Cl_{int} (μL/min/mg)
		1st	2nd	Mean	1st	2nd	Mean	
	15	100.0	100.0	100	115.5	70.5	93.0	74.5
	30	{75.0}	{44.8}					
	45	86.7	97.7	92				
	60	86.4	65.8	76				

*CL_{int}= 0.693/($t_{1/2}$*microsomal protein concentration)

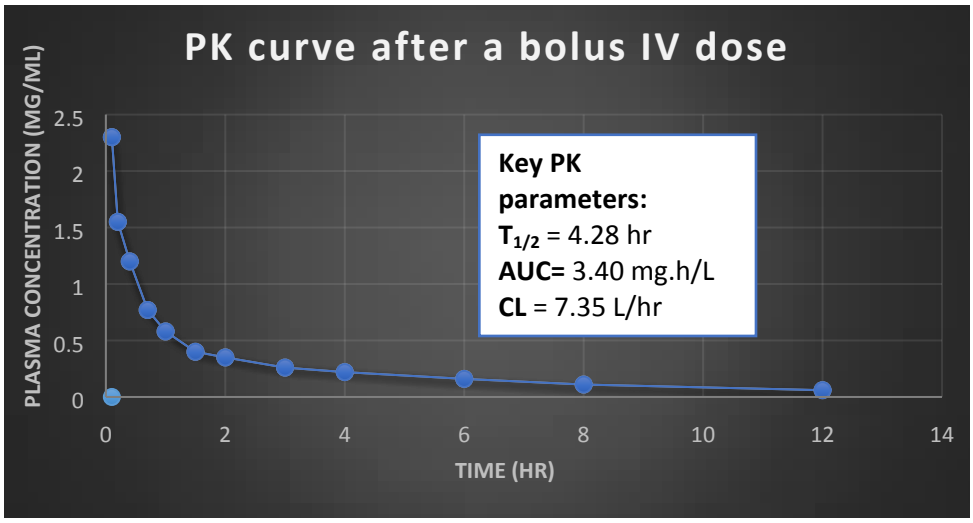

Figure 6. Pharmacokinetics (PK) curve (average of 3 animals), after a bolus IV dose, of compound **16**. $T_{1/2}$: half-life, Vβ: volume of distribution in the 2nd compartment, Cl: rate of clearance, AUC: area under the curve.

After testing the *in vitro* and *in vivo* pharmacokinetics of compound **16**, we moved towards investigating its mechanism of action. Originally, phenylthiazole scaffold restrains bacterial growth by perturbing the bacterial cell wall biosynthesis via inhibition of an essential enzyme called undecaprenyl diphosphate phosphatase (UppP).[26] Upon testing the UppP inhibition activity of compound **16**, it showed moderate inhibitory activity against UppP with an IC_{50} value of around 30 μM (Figure 7), which raises the point of having an additional bacterial target.

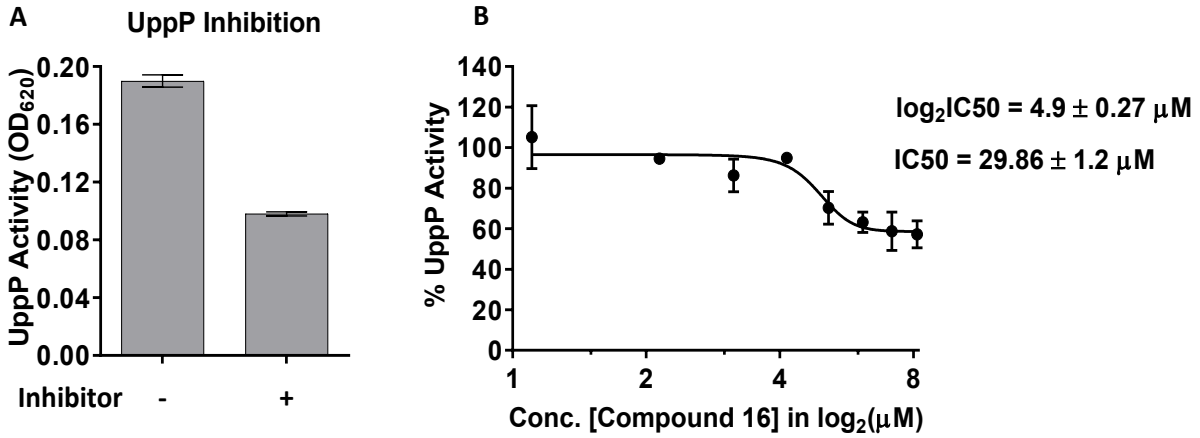

Figure 7. A) The activity of undecaprenyl diphosphate phosphatase (UppP) was measured by the release of inorganic phosphate in the absence of presence 283μM of the inhibitor, compound **16**. B) Dose-response curve for inhibition of undecaprenyl diphosphate phosphatase (UppP) by compound **16**. The activity of UppP was measured by the release of inorganic phosphate in the presence of an increasing concentrations of the inhibitor. Untreated sample with the reaction buffer only, served as a negative control (100% UppP activity). The results are presented as percent UppP inhibition, in presence of different concentrations of compound **16**, relative to the untreated samples. Error bars represent standard deviation values obtained from six measurements from three independent experiments.

Next, the promising *in vitro* activities of compound **16** led us to investigate its activity in an *in vivo* murine MRSA skin infection experiment. Mice were infected with MRSA USA300 and treated for 3 days with either petroleum jelly (PJ), petroleum jelly containing 2% compound **16**, or commercially available topical cream containing 2% fusidic acid (FA). Afterwards, wounds were harvested, homogenized and plated. Mice treated with petroleum jelly (PJ) only showed a significant skin lesion development that progressed to extensive skin damage until day 7 of the infection. Contrary to this, mice treated with PJ containing 2% of compound 16 significantly showed milder lesions and considerable skin healing by the end of the experiment. Bacterial colony counts from the drug-treated group were significantly lower than the PJ treated group (**$p \leq 0.01$), and considerably less systemic invasion as measured by colony counts in the spleens of infected

animals (Figure 8). The fusidic acid-treated control group showed slightly better lesion healing, less lesion colony counts, and less systemic involvement than the drug-treated group (Figure 8).

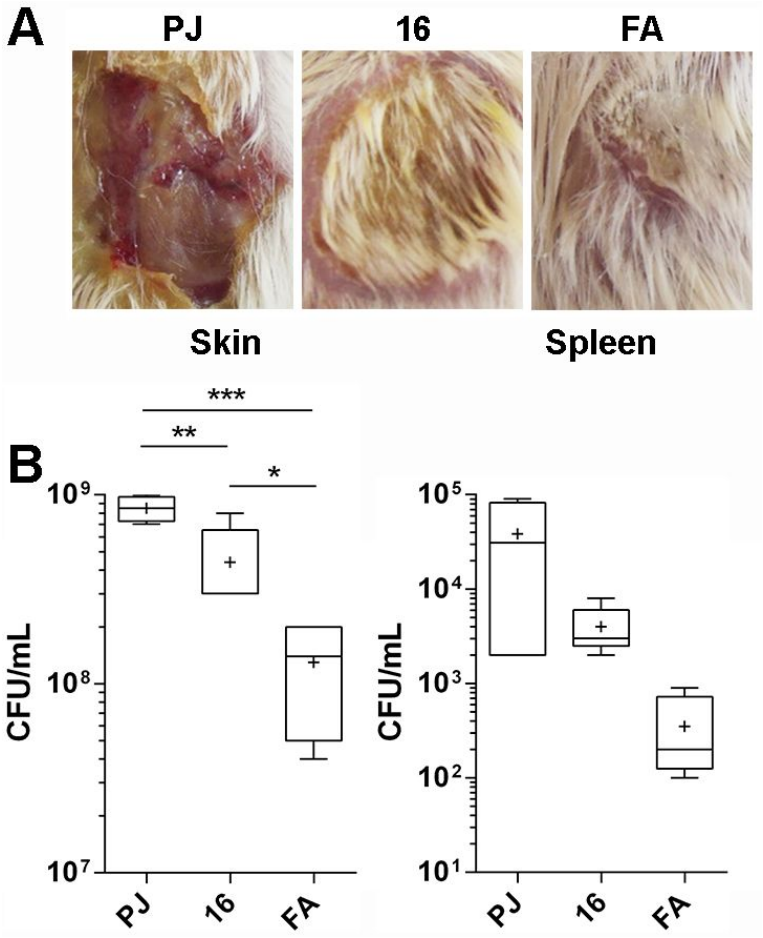

Figure 8. Compound 16 is active in vivo curing *S. aureus* skin infection in mice. Mice were infected subcutaneously with approximately 4 x 10^9 CFUs of *S. aureus* USA300. Within 72 h post-infection, an open wound/abscess was formed at the site of injection. Mice were then treated topically, twice daily for 4 days, with either petroleum jelly (PJ), 2% compound 16 in PJ (16) or a commercial cream with 2% fusidic acid (FA). **A.** Photographs of representative mice, on day 7, showing the infected and treated skin areas in the three groups. **B.** Box plots of the bacterial burden recovered from the skin lesions and spleens of the mice of the three groups. The whiskers span the difference between the minimum and maximum readings, the horizontal bar represents the median, and the (+) sign represents the mean of the CFU. Statistical analysis was done using One-way ANOVA followed by Tukey's multiple comparisons test**,** the * means $p \leq 0.05$, ** means $p \leq 0.01$, *** means $p \leq 0.001$, the charts were generated using GraphPad Prism.

Upon testing compound **16** in the *S. aureus* murine systemic model of infection, it was noticed that this compound, at a dose of 20 mg/kg, is capable of slightly lowering the mean

bacterial burdens in the kidneys of the mice as compared to the PBS group (Figure 9). At the same time, in the group treated with vancomycin (VA), at a dose of 50 mg/kg, the mean bacterial loads were lowered furthermore (Figure 9). The one-way ANOVA analysis of the three groups results showed a *p*-value of 0.0042. However, multiple comparisons (Tukey's test) between the three groups indicated that there were no significant differences between each two groups individually.

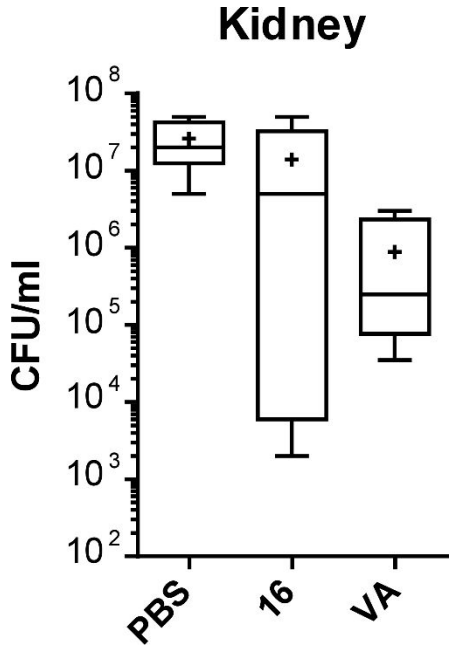

Figure 9. Box plots of the bacterial burden recovered from the kidneys of the mice of the three groups. The whiskers span the difference between the minimum and maximum readings, the horizontal bar represents the median, and the (+) sign represents the mean of the CFU/ml. Statistical analysis was done using One-way ANOVA followed by Tukey's multiple comparisons test**,** the chart was generated using GraphPad Prism.

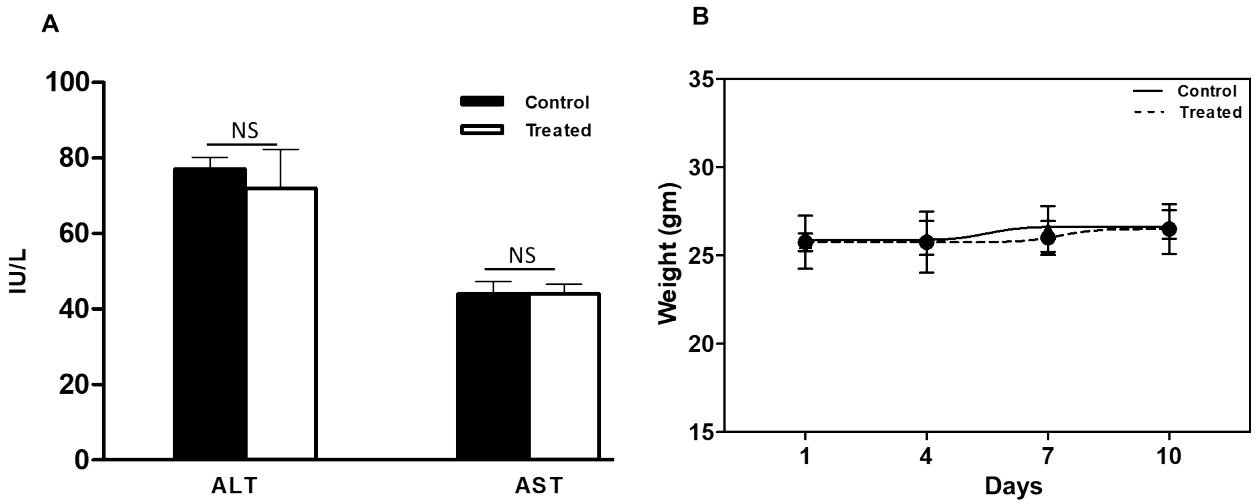

Figure (10). Acute toxicity study of compound **16** on male BALB/c mice; A) serum level of hepatic transaminases. B) Body weight over 10 days

Finally, the serum level of transaminases, as an indicator of hepatic injury, shows no significant increase as shown in Figure 10A, which indicates no liver toxicity after oral administration of up to 250 mg/kg. Furthermore, body weight shows no difference between control and treated animals after 1,4,7, and 10 days of oral administration of 250 mg/kg (Figure 10B).

Conclusion. The present study aimed at expanding our understanding of the SAR of phenylthiazole antibacterial scaffold, as a novel class of antibacterial agents. Through studying the basicity and the stereochemistry of the cationic side chain, it was found that the side chains with two amino groups possess superior antibacterial properties than their corresponding hydroxy-containing derivatives. The nullified antibacterial activity of all less basic amide-containing analogs strongly correlates the antibacterial activity with the basicity of the side chains. From the spatial arrangement point of view, incorporating the two terminal amino groups with cyclic or alicyclic structure provided disparity in antibacterial response. In this context, the piperidine-containing derivative **16** is over 32-times more potent against MRSA than the corresponding pyrrolidine-containing structure **15**. Compound **16** maintained its low MIC value (2 μg/mL)

against most of the additionally tested drug-resistant Gram-positive pathogens including vancomycin-resistant staphylococcal and enterococcal strains. Moreover, compound **16** possesses several additional attributes that make it worth considering as an antibiotic candidate. In brief, it has a rapid bactericidal mode of action, low potential of developing resistance, highly selective to prokaryotic cells over mammalian cells, and completely cleared the intracellular staphylococci burden. Initial pharmacokinetic analysis indicated the suitability of compound **16** for systemic invasive staphylococcal and enterococcal infections with a twice-daily dose-frequency. From a mechanistic point of view, compound **16** is a moderate inhibitor for undecaprenyl diphosphate phosphatase (UppP) with an IC_{50} value of about 30 μM. Lastly, compound **16** was found to significantly reduce MRSA burden *in vivo* in a MRSA murine skin infection experiment with no observable acute toxicity.

Methods

Chemistry

General. Melting points were obtained using a Stuart melting point apparatus and were uncorrected. Microanalyses for C, H, and N were performed at the Regional Center for Mycology and Biotechnology, Al-Azhar University. ^{1}H NMR spectra were recorded using a Bruker 400 MHz (Bruker Corp., Billerica, MA, USA) spectrophotometer at the Faculty of Pharmacy, Cairo University, Cairo, Egypt, and Varian Mercury-300BB 300 MHz (Varian Corp., Palo Alto, CA, USA) spectrophotometer at the Cairo University and Faculty of Science, Cairo University, Cairo, Egypt. Chemical shifts are given in parts per million (ppm) on the delta (δ) scale and coupling constants (J) were reported in Hz. Chemical shifts were calibrated relative to those of the solvents.[42] ^{13}C NMR spectra were recorded using a Bruker 100 MHz spectrophotometer at the Faculty of Pharmacy, Cairo University, Cairo, Egypt and Varian Mercury-300BB 75 MHz at the

Faculty of Science, Cairo University, Cairo, Egypt. The progress of the reactions was monitored with TLC using pre-coated aluminum sheet silica gel MERCK 60F 254. The spots were visualized using a UV lamp. The solvent system used for this assay was ethyl acetate: hexane [7:3] or [9:1]. All yields reported refer to isolated yields. Compounds 1-6 were prepared and characterized as reported elsewhere.[27]

Compounds 7-25. ***General procedure****.* To a solution of **6** (0.1 g, 0.25 mmol) in dry DMF (5 mL), a proper amine (0.4 mmol) was added. The reaction mixtures were heated at 80 °C for 4-8 h, and then poured over ice water (50 mL), the formed solid was filtered and washed with 50% ethanol and recrystallized from absolute ethanol to give the desired products. Physical properties and spectral analysis of all isolated products are listed below:

***N*-{4-[2-((1,1'-Biphenyl)-4-yl)-4-methylthiazol-5-yl]pyrimidin-2-yl}ethane-1,2-diamine (7)**

Following the general procedure, and using ethylenediamine (21 µL, 0.4 mmol), compound **7** was obtained as yellow solid (0.09 g, 94%) mp = 204 °C; ^{1}H NMR (DMSO-d_6) δ: 8.33 (d, J = 4.8 Hz, 1H), 8.03 (d, J = 8.4 Hz, 2H), 7.80 (d, J = 8.4 Hz, 2H), 7.72 (d, J = 7.2 Hz, 2H), 7.47 (t, J = 7.6 Hz, 2H), 7.39 (t, J = 6.8 Hz, 1H), 7.33 (brs, 1H), 6.86 (d, J = 4.8 Hz, 1H), 3.35- 3.31 (m, 2H), 2.71 (s, 3H), 2.65-2.60 (m, 2H), 1.67 (brs, 2H); ^{13}C NMR (DMSO-d_6) δ: 166.1, 162.5, 161.5, 153.5, 142.5, 139.4, 132.1, 129.5, 129.4, 128.5, 127.8, 127.19, 127.11, 127.0, 106.2, 38.7, 31.5, 18.6; HRMS (EI) *m/z* 387.5060 M^+, calcd for $C_{22}H_{21}N_5S$ 387.5050; Anal. Calc. for: ($C_{22}H_{21}N_5S$): C, 68.19; H, 5.46; N, 18.07%; Found: C, 68.28; H, 5.55; N, 18.15%.

***N*-{4-[2-((1,1'-Biphenyl)-4-yl)-4-methylthiazol-5-yl]pyrimidin-2-yl}propane-1,3-diamine (8)**

Following the general procedure, and using propane-1,3-diamine (27 µL, 0.4 mmol), compound **8** was obtained as yellow solid (0.09 g, 91%) mp = 165 °C; ^{1}H NMR (DMSO-d_6) δ: 8.34 (d, J = 4.8 Hz, 1H), 8.04 (d, J = 8.4 Hz, 2H), 7.81 (d, J = 8.4 Hz, 2H), 7.73 (d, J = 7.2 Hz, 2H), 7.48 (t, J =

7.6 Hz, 2H), 7.39 (t, *J* = 6.8 Hz, 1H), 7.24 (brs, 1H), 6.89 (d, *J* = 4.8 Hz, 1H), 3.20- 3.17 (m, 2H), 2.86- 2.85 (m, 2H), 2.71 (s, 3H), 2.30-2.28 (m, 2H), 1.17 (brs, 2H); ^{13}C NMR (DMSO-d_6) δ: 166.1, 162.6, 161.4, 159.3, 153.5, 142.5, 139.4, 132.1, 131.9, 129.5, 128.5, 127.8, 127.19, 127.12, 106.9, 44.4, 41.4, 35.0, 18.6; HRMS (EI) *m/z* 401.5318 M^+, calcd for $C_{23}H_{23}N_5S$ 401.5320; Anal. Calc. for: ($C_{23}H_{23}N_5S$): C, 68.80; H, 5.77; N, 17.44%; Found: C, 68.87; H, 5.85; N, 17.21%.

2-{[4-(2-((1,1'-Biphenyl)-4-yl)-4-methylthiazol-5-yl)pyrimidin-2-yl]amino}ethan-1-ol (9)

Following the general procedure, and using 2-aminoethan-1-ol (21 µL, 0.4 mmol), compound **9** was obtained as yellow solid (0.09 g, 94%) mp = 173 °C; ^{1}H NMR (DMSO-d_6) δ: 8.35 (d, *J* = 4.8 Hz, 1H), 8.04 (d, *J* = 8.4 Hz, 2H), 7.82 (d, *J* = 8.4 Hz, 2H), 7.73 (d, *J* = 7.2 Hz, 2H), 7.48 (t, *J* = 7.6 Hz, 2H), 7.39 (t, *J* = 6.8 Hz, 1H), 7.13 (brs, 1H), 6.90 (d, *J* = 4.8 Hz, 1H), 4.68 (brs, 1H), 3.55-3.54 (m, 2H), 3.40- 3.35 (m, 2H), 2.72 (s, 3H); ^{13}C NMR (DMSO-d_6) δ: 166.1, 162.5, 159.4, 157.2, 153.6, 142.5, 139.4, 132.1, 131.9, 129.5, 128.5, 127.8, 127.2, 127.1, 106.5, 60.0, 43.9, 18.6; HRMS (EI) *m/z* 388.4909 M^+, calcd for $C_{22}H_{20}N_4OS$ 388.4890; Anal. Calc. for: ($C_{22}H_{20}N_4OS$): C, 68.02; H, 5.19; N, 14.42%; Found: C, 68.09; H, 5.26; N, 14.49%.

3-{[4-(2-((1,1'-Biphenyl)-4-yl)-4-methylthiazol-5-yl)pyrimidin-2-yl]amino}propan-1-ol (10)

Following the general procedure , and using 3-aminopropan-1-ol (27 µL, 0.4 mmol), compound **10** was obtained as yellow solid (0.09 g, 86%) mp = 113°C; ^{1}H NMR (DMSO-d_6) δ: 8.34 (d, *J* = 4.8 Hz, 1H), 8.04 (d, *J* = 8.4 Hz, 2H), 7.81 (d, *J* = 8.4 Hz, 2H), 7.73 (d, *J* = 7.2 Hz, 2H), 7.48 (t, *J* = 7.6 Hz, 2H), 7.39 (t, *J* = 6.8 Hz, 1H), 7.23 (brs, 1H), 6.88 (d, *J* = 4.8 Hz, 1H), 4.51 (brs, 1H), 3.50- 3.45 (m, 2H), 3.37- 3.34 (m, 2H), 2.72 (s, 3H), 1.70 (t, *J* = 6 Hz, 2H); ^{13}C NMR (DMSO-d_6) δ: 166.1, 162.5, 159.4, 157.2, 153.5, 142.5, 139.4, 132.1, 131.9, 129.5, 128.5, 127.8, 127.2, 127.12, 106.5, 59.1, 38.5, 32.5, 18.6; HRMS (EI) *m/z* 402.5164 M^+, calcd for $C_{23}H_{22}N_4OS$ 402.5160; Anal. Calc. for: ($C_{23}H_{22}N_4OS$): C, 68.63; H, 5.51; N, 13.92%; Found: C, 68.73; H, 5.59; N, 13.99%.

1-{[4-(2-((1,1'-Biphenyl)-4-yl)-4-methylthiazol-5-yl)pyrimidin-2-yl]amino}ethane-1,2-diol (11). Following the general procedure, and using 3-aminopropane-1,2-diol (33 μL, 0.4 mmol), compound **11** was obtained as yellow solid (0.07 g, 63%) mp = 176 °C; ^{1}H NMR (DMSO-d_6) δ: 8.34 (d, J = 4.8 Hz, 1H), 8.04 (d, J = 8.4 Hz, 2H), 7.81 (d, J = 8.4 Hz, 2H), 7.73 (d, J = 7.2 Hz, 2H), 7.46 (t, J = 7.6 Hz, 2H), 7.41 (t, J = 6.8 Hz, 1H), 7.01 (brs, 1H), 6.90 (d, J = 4.8 Hz, 1H), 4.76 (brs, 1H), 4.54 (brs, 1H), 3.88- 3.67 (m, 1H), 3.44- 3.37 (m, 2H), 3.15- 3.13 (m, 2H), 2.71 (s, 3H); ^{13}C NMR (DMSO-d_6) δ: 166.3, 162.5, 159.4, 157.6, 153.6, 142.5, 139.4, 132.1, 131.9, 129.5, 128.5, 127.8, 127.2, 127.1, 106.5, 70.6, 64.5, 44.8, 18.6; HRMS (EI) *m/z* 418.5153 M^+, calcd for $C_{23}H_{22}N_4O_2S$ 418.5150; Anal. Calc. for: ($C_{23}H_{22}N_4O_2S$): C, 66.01; H, 5.30; N, 13.39%; Found: C, 66.09; H, 5.38; N, 13.47%.

(*R*)-1-{[4-(2-((1,1'-Biphenyl)-4-yl)-4-methylthiazol-5-yl)pyrimidin-2-yl]amino}ethane-1,2-diol (12). Following the general procedure, and using (*R*)-3-aminopropane-1,2-diol (33 mg, 0.4 mmol), compound **12** was obtained as yellow solid (0.06 g, 57%) mp = 166 °C; ^{1}H NMR (DMSO-d_6) δ: 8.34 (d, J = 4.8 Hz, 1H), 8.04 (d, J = 8.4 Hz, 2H), 7.81 (d, J = 8.4 Hz, 2H), 7.73 (d, J = 7.2 Hz, 2H), 7.48 (t, J = 7.6 Hz, 2H), 7.41 (t, J = 6.8 Hz, 1H), 7.01 (brs, 1H), 6.90 (d, J = 4.8 Hz, 1H), 4.77 (brs, 1H), 4.55 (brs, 1H), 3.69- 3.68 (m, 1H), 3.41- 3.38 (m, 2H), 3.23- 3.20 (m, 2H), 2.71 (s, 3H); ^{13}C NMR (DMSO-d_6) δ: 166.2, 162.5, 159.4, 157.2, 153.6, 142.5, 139.4, 132.1, 131.6, 129.5, 128.5, 127.8, 127.2, 127.1, 106.2, 70.6, 64.5, 44.8, 18.7; HRMS (EI) *m/z* 418.5142 M^+, calcd for $C_{23}H_{22}N_4O_2S$ 418.5150; Anal. Calc. for: ($C_{23}H_{22}N_4O_2S$): C, 66.01; H, 5.30; N, 13.39%; Found: C, 66.12; H, 5.39; N, 13.44%.

(*S*)-3-{[4-(2-((1,1'-Biphenyl)-4-yl)-4-methylthiazol-5-yl)pyrimidin-2-yl]amino}propane-1,2-diol (13). Following the general procedure, and using (*S*)-3-aminopropane-1,2-diol (33 mg, 0.4 mmol), compound **13** was obtained as yellow solid (0.07 g, 75%) mp = 164 °C; ^{1}H NMR (DMSO-

d_6) δ: 8.35 (d, J = 4.8 Hz, 1H), 8.05 (d, J = 8.4 Hz, 2H), 7.82 (d, J = 8.4 Hz, 2H), 7.74 (d, J = 7.2 Hz, 2H), 7.49 (t, J = 7.6 Hz, 2H), 7.40 (t, J = 6.8 Hz, 1H), 7.01 (brs, 1H), 6.91 (d, J = 4.8 Hz, 1H), 4.77 (brs, 1H), 4.53 (brs, 1H), 3.73- 3.68 (m, 1H), 3.38- 3.30 (m, 2H), 3.28- 3.20 (m, 2H), 2.73 (s, 3H); ^{13}C NMR (DMSO-d_6) δ: 166.2, 162.5, 159.3, 157.6, 153.6, 142.5, 139.4, 132.1, 131.9, 129.5, 128.5, 127.9, 127.2, 127.1, 106.2, 70.6, 64.5, 44.8, 18.6; HRMS (EI) *m/z* 418.5166 M^+, calcd for $C_{23}H_{22}N_4O_2S$ 418.5150; Anal. Calc. for: ($C_{23}H_{22}N_4O_2S$): C, 66.01; H, 5.30; N, 13.39%; Found: C, 66.07; H, 5.36; N, 13.47%.

2-{[4-(2-((1,1'-biphenyl)-4-yl)-4-methylthiazol-5-yl)pyrimidin-2-yl]amino}propane-1,3-diol (14). Following the general procedure, and using 2-aminopropane-1,3-diol (33 mg, 0.4 mmol), compound **14** was obtained as yellow solid (0.08 g, 81%) mp = 154 °C; ^{1}H NMR (DMSO-d_6) δ: 8.36 (d, J = 4.8 Hz, 1H), 8.04 (d, J = 8.4 Hz, 2H), 7.82 (d, J = 8.4 Hz, 2H), 7.73 (d, J = 7.2 Hz, 2H), 7.48 (t, J = 7.6 Hz, 2H), 7.39 (t, J = 6.8 Hz, 1H), 6.90 (d, J = 4.8 Hz, 1H), 6.67 (brs, 1H), 4.62 (brs, 2H), 3.95 (p, J = 6 Hz, 1H), 3.15- 3.13 (m, 4H), 2.72 (s, 3H); ^{13}C NMR (DMSO-d_6) δ: 166.1, 162.3, 159.3, 157.6, 153.6, 142.5, 139.4, 132.1, 129.5, 128.5, 127.8, 127.2, 127.19, 127.13, 106.5, 60.6, 55.0, 18.3; HRMS (EI) *m/z* 418.5137 M^+, calcd for $C_{23}H_{22}N_4O_2S$ 418.5150; Anal. Calc. for: ($C_{23}H_{22}N_4O_2S$): C, 66.01; H, 5.30; N, 13.39%; Found: C, 66.09; H, 5.38; N, 13.43%.

4-{2-[(1,1'-biphenyl)-4-yl]-4-methylthiazol-5-yl}-*N*-(pyrrolidin-3-yl)pyrimidin-2-amine (15) Following the general procedure, using 3-amino-pyrrolidine dihydrochloride (60 mg, 0.4 mmol) and potassium carbonate anhydrous (0.1 g, 0.7 mmol), compound **15** was obtained as orange solid (0.1 g, 98%) mp = 90 °C; ^{1}H NMR (DMSO-d_6) δ: 8.37 (d, J = 4.8 Hz, 1H), 8.02 (d, J = 8.4 Hz, 2H), 7.93 (brs, 1H), 7.79 (d, J = 8.4 Hz, 2H), 7.71 (d, J = 7.2 Hz, 2H), 7.47 (t, J = 7.6 Hz, 2H), 7.38 (t, J = 6.8 Hz, 1H), 6.85 (d, J = 4.8 Hz, 1H), 3.62- 3.28 (m, 3H), 2.73 (s, 3H), 2.03- 1.98 (m, 2H), 1.72- 1.70 (m, 2H), 1.18 (brs, 1H); ^{13}C NMR (DMSO-d_6) δ: 166.1, 160.1, 159.2, 157.8, 153.7,

142.5, 139.4, 132.1, 131.9, 129.5, 128.5, 127.8, 127.18, 127.10, 106.0, 54.8, 51.0, 45.2, 34.0, 18.7; HRMS (EI) *m/z* 413.5436 M^+, calcd for $C_{24}H_{23}N_5S$ 413.5430; Anal. Calc. for: ($C_{24}H_{23}N_5S$): C, 69.71; H, 5.61; N, 16.94%; Found: C, 69.79; H, 5.71; N, 17.04%.

4-{2-[(1,1'-biphenyl)-4-yl]-4-methylthiazol-5-yl}-*N*-(piperidin-2-ylmethyl)pyrimidin-2-amine (16). Following the general procedure, and using 2-(aminomethyl)piperidine (42 μL, 0.4 mmol), compound **16** was obtained as yellow solid (0.1 g, 94%) mp = 146 °C; ^{1}H NMR (DMSO-d_6) δ: 8.38 (d, *J* = 4.8 Hz, 1H), 8.05 (d, *J* = 8.4 Hz, 2H), 7.82 (d, *J* = 8.4 Hz, 2H), 7.74 (d, *J* = 7.2 Hz, 2H), 7.51 (t, *J* = 7.6 Hz, 2H), 7.40 (t, *J* = 6.8 Hz, 1H), 7.20 (brs, 1H), 6.89 (d, *J* = 4.8 Hz, 1H), 3.31- 3.15 (m, 2H), 2.93- 2.91 (m, 2H), 2.72 (s, 3H), 2.63- 2.60 (m, 1H), 1.75- 1.23 (m, 6H), 1.02 (brs, 1H); ^{13}C NMR (DMSO-d_6) δ: 166.1, 162.6, 159.4, 157.2, 153.6, 142.5, 139.4, 132.1, 131.9, 129.5, 128.5, 127.8, 127.19, 127.13, 106.2, 56.2, 47.2, 46.6, 30.7, 26.5, 24.7, 18.6; HRMS (EI) *m/z* 441.5971 M^+, calcd for $C_{26}H_{27}N_5S$ 441.5970; Anal. Calc. for: ($C_{26}H_{27}N_5S$): C, 70.72; H, 6.16; N, 15.86%; Found: C, 70.83; H, 6.25; N, 15.93%.

***N*-{4-[2-((1,1'-Biphenyl)-4-yl)-4-methylthiazol-5-yl]pyrimidin-2-yl}cyclohexane-*trans*-1,4-diamine (17).** Following the general procedure, and using *trans*-1,4-diaminocyclohexane (42 mg, 0.4 mmol), compound **17** was obtained as yellow solid (0.1 g, 97%) mp = 260 °C; ^{1}H NMR (DMSO-d_6) δ: 8.34 (d, *J* = 4.8 Hz, 1H), 8.06 (d, *J* = 8.4 Hz, 2H), 7.82 (d, *J* = 8.4 Hz, 2H), 7.74 (d, *J* = 7.2 Hz, 2H), 7.49 (t, *J* = 7.6 Hz, 2H), 7.40 (t, *J* = 6.8 Hz, 1H), 7.13 (brs, 1H), 6.91 (d, *J* = 4.8 Hz, 1H), 3.72- 3.55 (m, 2H), 2.74 (s, 3H), 1.97-1.87 (m, 4H), 1.33-1.28 (m, 4H), 1.20 (brs, 2H); ^{13}C NMR (DMSO-d_6) δ: 166.3, 161.8, 159.7, 157.6, 153.1, 142.5, 139.4, 132.1, 131.9, 129.5, 128.5, 127.9, 127.16, 127.13, 106.5, 49.6, 37.1, 33.3, 31.2, 30.5, 18.6; HRMS (EI) *m/z* 441.5951 M^+, calcd for $C_{26}H_{27}N_5S$ 441.5970; Anal. Calc. for: ($C_{26}H_{27}N_5S$): C, 70.72; H, 6.16; N, 15.86%; Found: C, 70.83; H, 6.25; N, 15.94%.

***N*-{4-[2-((1,1'-Biphenyl)-4-yl)-4-methylthiazol-5-yl]pyrimidin-2-yl}cyclohexane-*cis*-1,2-diamine (18).** Following the general procedure, and using (±)-*cis*-1,2-diaminocyclohexane (42 µL, 0.4 mmol), compound **18** was obtained as brown solid (0.06 g, 51%) mp = 104 °C; ^{1}H NMR (DMSO-d_6) δ: 8.36 (d, J = 4.8 Hz, 1H), 8.06 (d, J = 8.4 Hz, 2H), 7.85 (d, J = 8.4 Hz, 2H), 7.72 (d, J = 7.2 Hz, 2H), 7.47 (t, J = 7.6 Hz, 2H), 7.42 (t, J = 6.8 Hz, 1H), 6.91 (d, J = 4.8 Hz, 1H), 4.65 (brs, 1H), 4.03- 3.86 (m, 2H), 3.11- 3.08 (m, 2H), 2.71 (s, 3H), 1.90-1.28 (m, 6H), 1.20 (brs, 2H); ^{13}C NMR (DMSO-d_6) δ: 166.3, 161.8, 159.0, 157.6, 153.8, 142.5, 139.4, 132.1, 129.5, 128.5, 127.8, 127.2, 127.19, 127.13, 105.5, 54.5, 49.3, 39.3, 26.4, 21.21, 19.7, 18.6; HRMS (EI) *m/z* 441.5955 M^+, calcd for $C_{26}H_{27}N_5S$ 441.5970; Anal. Calc. for: ($C_{26}H_{27}N_5S$): C, 70.72; H, 6.16; N, 15.86%; Found: C, 70.81; H, 6.25; N, 15.93%.

***N*-{4-[2-((1,1'-biphenyl)-4-yl)-4-methylthiazol-5-yl]pyrimidin-2-yl}cyclohexane-*trans*-1,2-diamine (19).** Following the general procedure, and using (±)-*trans*-1,2-Diaminocyclohexane (42 µL, 0.4 mmol), compound **19** was obtained as brown solid (0.1 g, 94%) mp = 93 °C; ^{1}H NMR (DMSO-d_6) δ: 8.33 (d, J = 4.8 Hz, 1H), 8.03 (d, J = 8.4 Hz, 2H), 7.82 (d, J = 8.4 Hz, 2H), 7.73 (d, J = 7.2 Hz, 2H), 7.48 (t, J = 7.6 Hz, 2H), 7.39 (t, J = 6.8 Hz, 1H), 7.14 (brs, 1H), 6.86 (d, J = 4.8 Hz, 1H), 3.48- 3.46 (m, 2H), 3.30- 3.15 (m, 2H), 2.72 (s, 3H), 2.05-1.08 (m, 2H), 1.64 (brs, 2H), 1.23-1.10 (m, 4H); ^{13}C NMR (DMSO-d_6) δ: 166.0, 162.7, 159.4, 157.6, 153.5, 142.5, 139.4, 132.3, 132.1, 129.5, 128.5, 127.9, 127.18, 127.12, 106.9, 53.7, 37.1, 34.9, 31.2, 25.3, 25.2, 18.6; HRMS (EI) *m/z* 441.5981 M^+, calcd for $C_{26}H_{27}N_5S$ 441.5970; Anal. Calc. for: ($C_{26}H_{27}N_5S$): C, 70.72; H, 6.16; N, 15.86%; Found: C, 70.81; H, 6.23; N, 15.95%.

(*R*)-{1-[4-(2-((1,1'-Biphenyl)-4-yl)-4-methylthiazol-5-yl)pyrimidin-2-yl]pyrrolidin-2-yl}methanol (20). Following the general procedure, using (*R*)-(+)-2-pyrrolidinemethanol (37 µL, 0.4 mmol), compound **20** was obtained as yellow solid (0.1 g, 96%) mp = 105 °C; ^{1}H NMR

(DMSO-d_6) δ: 8.40 (d, J = 4.8 Hz, 1H), 8.04 (d, J = 8.4 Hz, 2H), 7.81 (d, J = 8.4 Hz, 2H), 7.73 (d, J = 7.2 Hz, 2H), 7.48 (t, J = 7.6 Hz, 2H), 7.39 (t, J = 6.8 Hz, 1H), 6.91 (d, J = 4.8 Hz, 1H), 4.76 (brs, 1H), 4.18- 4.12 (m, 1H), 3.68- 3.66 (m, 2H), 3.53- 3.47 (m, 2H), 2.71 (s, 3H), 2.03- 1.89 (m, 4H); ^{13}C NMR (DMSO-d_6) δ: 166.2, 160.2, 158.6, 153.4, 142.5, 139.4, 132.3, 131.6, 129.5, 128.5, 128.1, 127.8, 127.2, 127.1, 106.3, 60.7, 59.4, 47.7, 28.0, 22.9, 18.7; HRMS (EI) *m/z* 428.5549 M^+, calcd for $C_{25}H_{24}N_4OS$ 428.5540; Anal. Calc. for: ($C_{25}H_{24}N_4OS$): C, 70.07; H, 5.65; N, 13.07%; Found: C, 70.18; H, 5.73; N, 13.16%.

(*S*)-{1-[4-(2-((1,1'-Biphenyl)-4-yl)-4-methylthiazol-5-yl)pyrimidin-2-yl]pyrrolidin-2-yl}methanol (21). Following the general procedure, using (*S*)-(-)-2-pyrrolidinemethanol (37 µL, 0.4 mmol), compound **21** was obtained as grey solid (0.09 g, 87%) mp = 256 °C; ^{1}H NMR (DMSO-d_6) δ: 8.39 (d, J = 4.8 Hz, 1H), 8.04 (d, J = 8.4 Hz, 2H), 7.81 (d, J = 8.4 Hz, 2H), 7.73 (d, J = 7.2 Hz, 2H), 7.48 (t, J = 7.6 Hz, 2H), 7.39 (t, J = 6.8 Hz, 1H), 6.90 (d, J = 4.8 Hz, 1H), 4.80 (brs, 1H), 4.12- 4.11 (m, 1H), 3.65- 3.53 (m, 2H), 3.48- 3.43 (m, 2H), 2.73 (s, 3H), 2.02- 1.88 (m, 4H); ^{13}C NMR (DMSO-d_6) δ: 166.2, 160.2, 159.0, 157.6, 153.1, 142.5, 139.4, 132.3, 132.1, 129.5, 128.5, 127.8, 127.2, 127.1, 106.3, 60.7, 59.7, 47.7, 28.0, 22.9, 18.7; HRMS (EI) *m/z* 428.5542 M^+, calcd for $C_{25}H_{24}N_4OS$ 428.5540; Anal. Calc. for: ($C_{25}H_{24}N_4OS$): C, 70.07; H, 5.65; N, 13.07%; Found: C, 70.13; H, 5.69; N, 13.11%.

(*R*)-1-{4-[2-((1,1'-biphenyl)-4-yl)-4-methylthiazol-5-yl]pyrimidin-2-yl}-*N*,*N*-dimethylpyrrolidin-3-amine (22). Following the general procedure, using (*R*)-(+)-3-(dimethylamino)pyrrolidine dihydrochloride (71 mg, 0.4 mmol) and potassium carbonate anhydrous (0.1 g, 0.7 mmol), compound **22** was obtained as yellow solid (0.1 g, 91%) mp = 127 °C; ^{1}H NMR (DMSO-d_6) δ: 8.38 (d, J = 4.8 Hz, 1H), 8.02 (d, J = 8.4 Hz, 2H), 7.78 (d, J = 8.4 Hz, 2H), 7.72 (d, J = 7.2 Hz, 2H), 7.47 (t, J = 7.6 Hz, 2H), 7.39 (t, J = 6.8 Hz, 1H), 6.87 (d, J = 4.8 Hz,

1H), 3.80- 3.68 (m, 3H), 3.41- 3.37 (m, 2H), 3.18- 3.14 (m, 1H), 2.73 (s, 3H), 2.18 (s, 6H), 1.81- 1.75 (m, 1H); ^{13}C NMR (DMSO-d_6) δ: 166.1, 159.9, 159.2, 157.9, 153.8, 142.5, 139.4, 132.1, 132.0, 129.5, 128.5, 127.8, 127.19, 127.11, 106.2, 65.1, 50.9, 45.9, 44.2, 29.8, 18.7; HRMS (EI) *m/z* 441.6013 M^+, calcd for $C_{26}H_{27}N_5S$ 441.6020; Anal. Calc. for: ($C_{26}H_{27}N_5S$): C, 70.72; H, 6.16; N, 15.86%; Found: C, 70.80; H, 6.23; N, 15.94%.

(*S*)-1-{4-[2-((1,1'-biphenyl)-4-yl)-4-methylthiazol-5-yl]pyrimidin-2-yl}-*N*,*N*-dimethylpyrrolidin-3-amine (23). Following the general procedure, and using (*S*)-(-)-3-(dimethylamino)pyrrolidine (42 μL, 0.4 mmol), compound **23** was obtained as yellow solid (0.07 g, 64%) mp = 136 °C; ^{1}H NMR (DMSO-d_6) δ: 8.39 (d, J = 4.8 Hz, 1H), 8.03 (d, J = 8.4 Hz, 2H), 7.79 (d, J = 8.4 Hz, 2H), 7.72 (d, J = 7.2 Hz, 2H), 7.48 (t, J = 7.6 Hz, 2H), 7.39 (t, J = 6.8 Hz, 1H), 6.89 (d, J = 4.8 Hz, 1H), 3.80- 3.71 (m, 3H), 3.45- 3.38 (m, 2H), 3.20- 3.10 (m, 1H), 2.73 (s, 3H), 2.19 (s, 6H), 1.81- 1.79 (m, 1H); ^{13}C NMR (DMSO-d_6) δ: 166.1, 159.9, 159.2, 157.9, 153.8, 142.5, 139.4, 132.1, 132.0, 129.5, 128.5, 127.8, 127.2, 127.1, 106.2, 65.3, 51.0, 45.9, 44.3, 29.8, 18.7; HRMS (EI) *m/z* 441.6006 M^+, calcd for $C_{26}H_{27}N_5S$ 441.6020; Anal. Calc. for: ($C_{26}H_{27}N_5S$): C, 70.72; H, 6.16; N, 15.86%; Found: C, 70.78; H, 6.24; N, 15.92%.

(*R*)-1-{4-[2-((1,1'-biphenyl)-4-yl)-4-methylthiazol-5-yl]pyrimidin-2-yl}pyrrolidine-2-carboxamide (24). Following the general procedure, using D-prolinamide (42 mg, 0.4 mmol), compound **24** was obtained as yellow solid (0.1 g, 92%) mp = 229 °C; ^{1}H NMR (DMSO-d_6) δ: 8.42 (d, J = 4.8 Hz, 1H), 8.05 (d, J = 8.4 Hz, 2H), 7.83 (d, J = 8.4 Hz, 2H), 7.75 (d, J = 7.2 Hz, 2H), 7.47 (t, J = 7.6 Hz, 2H), 7.40 (t, J = 6.8 Hz, 1H), 6.95 (d, J = 4.8 Hz, 1H), 6.86 (brs, 2H), 4.41- 4.33 (m, 1H), 3.68- 3.59 (m, 2H), 2.71 (s, 3H), 2.21- 2.17 (m, 1H), 1.98- 1.93 (m, 3H); ^{13}C NMR (DMSO-d_6) δ: 174.9, 166.3, 160.4, 159.7, 157.2, 153.4, 142.5, 139.4, 132.2, 129.5, 128.5, 128.1, 127.8, 127.4, 127.1, 106.7, 60.6, 47.6, 31.1, 23.6, 18.6; HRMS (EI) *m/z* 441.5531 M^+, calcd

for $C_{25}H_{23}N_5OS$ 441.5530; Anal. Calc. for: ($C_{25}H_{23}N_5OS$): C, 68.00; H, 5.25; N, 15.86%; Found: C, 68.08; H, 5.31; N, 15.92%.

(*S*)-1-{4-[2-((1,1'-biphenyl)-4-yl)-4-methylthiazol-5-yl]pyrimidin-2-yl}pyrrolidine-2-carboxamide (25). Following the general procedure, using L-prolinamide (42 mg, 0.4 mmol), compound **25** was obtained as yellow solid (0.08 g, 74%) mp = 223 °C; ^{1}H NMR (DMSO-d_6) δ: 8.41 (d, J = 4.8 Hz, 1H), 8.02 (d, J = 8.4 Hz, 2H), 7.83 (d, J = 8.4 Hz, 2H), 7.72 (d, J = 7.2 Hz, 2H), 7.48 (t, J = 7.6 Hz, 2H), 7.40 (t, J = 6.8 Hz, 1H), 6.98 (d, J = 4.8 Hz, 1H), 6.87 (brs, 2H), 4.41- 4.39 (m, 1H), 3.70- 3.58 (m, 2H), 2.73 (s, 3H), 2.21- 1.92 (m, 1H), 1.96- 1.92 (m, 3H); ^{13}C NMR (DMSO-d_6) δ: 175.1, 166.3, 160.0, 159.2, 157.2, 153.8, 142.5, 139.4, 132.1, 129.5, 128.5, 127.8, 127.5, 127.4, 127.1, 106.7, 60.6, 47.6, 31.1, 23.6, 18.6; HRMS (EI) *m/z* 441.5535 M^+, calcd for $C_{25}H_{23}N_5OS$ 441.5530; Anal. Calc. for: ($C_{25}H_{23}N_5OS$): C, 68.00; H, 5.25; N, 15.86%; Found: C, 68.11; H, 5.34; N, 15.93%.

Microbiological assays

Bacterial strains, cell lines, media and reagents. The bacterial strains used in this study were obtained from the Biodefense and Emerging Infections Research Resources Repository (BEI Resources) and the American Type Culture Collection (ATCC). The human colorectal adenocarcinoma (Caco-2) cell line, human keratinocyte cell line (HaCaT), and murine macrophage (J774) cells were purchased from the American Type Culture Collection (ATCC). Linezolid and vancomycin hydrochloride were purchased from commercial vendors and dissolved either in sterile water or in DMSO to prepare stock solutions. Cation-adjusted Mueller Hinton broth (CA-MHB), tryptic soy agar (TSA), tryptic soy broth (TSB), phosphate-buffered saline (PBS), Dulbecco's Modified Eagle's Medium (DMEM), fetal bovine serum (FBS) and 96-well plates

were all purchased from commercial sources. Synthesized compounds were prepared in DMSO at stock concentrations of 10 mg/mL.

MICs and MBCs of tested compounds against *Staphylococcus aureus* and important Gram-positive bacterial pathogens. The minimum inhibitory concentration (MIC) of tested compounds and control antibiotics was determined using the broth microdilution method according to the guidelines outlined by the Clinical and Laboratory Standards Institute (CLSI).[43] See SI for detailed procedure.

Time-killing assay against MRSA. A time to kill assay was performed against MRSA USA 400 to confirm the bactericidal activity of the tested compounds, as described previously.[20] MRSA USA400 cells in the logarithmic growth phase were diluted to 4.7×10^6 colony-forming units (CFU/mL) and exposed to concentrations equivalent to 5 × MIC (in triplicate) of compounds **19** and **16** and vancomycin in tryptic soy broth. Aliquots (100 μL) were collected from each treatment at the indicated time points, subsequently serially diluted in PBS and plated on tryptic soy agar plates. Plates were incubated at 37°C for 18-20 h before the viable CFU/mL was determined.

***In vitro* analysis of the cytotoxicity toward Caco-2, HaCaT and J774 cells.** As described in previous a report.[44] All tested compounds were incubated with human colorectal cells (Caco-2), human keratinocytes (HaCaT) (for 2 hours) and murine macrophages (J774) (for 24 hours) to determine the potential toxicity toward mammalian cells. Detailed procedure is included in the SI.

Multi-step resistance study against MRSA. The ability of MRSA USA400 to develop resistance to the new derivatives was investigated via a multi-step resistance study, as described previously.[27, 45] Bacteria were serially passaged over a 14-day period and the broth microdilution assay was used to determine the MIC of each test agent against MRSA after each successive passage. Resistance was defined as a greater than four-fold increase from the initial MIC.[46]

Intracellular infection of J774 cells with MRSA and treatment with compounds 16 and 19. The ability of tested compounds to reduce the burden of intracellular MRSA was evaluated utilizing previously described methods.[44, 47] Detailed procedure is included in the SI.

Pharmacokinetic assays

Human Microsomal Stability Analysis. The metabolic stability of compound **16** to the hepatic metabolism was analyzed with pooled human liver microsomes as described previously.[17] The tested compounds were incubated in duplicates with human liver microsomes (pooled from human donors) at 37 ºC. The reaction contained microsomal protein in 100 mM potassium phosphate, 2 mM NADPH, 3 mM $MgCl_2$, pH 7.4. A control was run for each test agent omitting NADPH to detect NADPH-free degradation. At 0, 15, 30, 45, and 60 minutes, an aliquot was removed from each experimental and control reaction and mixed with an equal volume of ice-cold stop solution (methanol containing haloperidol, diclofenac, or other internal standard). Stopped reactions are incubated at least ten minutes at -20 ºC, and an additional volume of water was added. The samples were centrifuged to remove precipitated protein, and the supernatants were analyzed by LC/MS/MS to quantitate the remaining parent. Data are converted to % remaining by dividing by the time zero concentration value. Data are fit to a first-order decay model to determine half-life. Intrinsic clearance is calculated from the half-life and the protein concentrations: $CL_{int} = \ln(2) / (T_{1/2}$ [microsomal protein]).

***In vivo* Pharmacokinetics.** Pharmacokinetic studies were performed in male naïve Sprague–Dawley (SD) rats (three animals) following Institutional Animal Care and Use Committee guidelines, as described in a previous report.[28] In brief, an IV bolus of a 5 mg/Kg was directly administered. Blood samples were collected over a 12-hour period post-dose into Vacutainer tubes containing EDTA-K2. Plasma was isolated, and the concentration of tested compounds in plasma

was determined with LC/MS/MS after protein precipitation with acetonitrile. Two-compartmental pharmacokinetic analysis was performed on plasma concentration data in order to calculate pharmacokinetic parameters as previously reported.[18]

Biochemical assays

Protein Purification. *E. Coli* UppP in pET28a with a 6X His tag was expressed and purified using affinity chromatography as described in previous reports.[44] Briefly, transformed C41 (DE3) cells were grown exponentially in 2xYT media, induced with 1 mM IPTG at OD_{600} 0.7, and expressed overnight at 22°C. Harvested cells were washed with STE buffer (10 mM Tris-HCl (pH 8.0), 0.1 mM EDTA, 0.1 M NaCl), and resuspended in buffer A (25 mM Tris-HCl (pH 7.2), 150 mM NaCl, 5 mM 2-mercaptoethanol, 10% glycerol (v/v)). Cells were disrupted by sonication in the presence of 75 U MNase and 1 mM $CaCl_2$, and cell pellets were collected by centrifuged at 10,000 RPM for 30 minutes. Membrane extracts were washed once with buffer A, and then suspended in buffer A with 1.5% (w/v) DDM. This mixture was incubated overnight at 4°C with end-over-end rotation. The second centrifugation yielded a soluble extract which was further used for purification. The soluble extract was incubated at 4°C for 3 hours with 0.75 mL of Ni-NTA equilibrated with buffer B (25 mM Tris-HCl (pH 7.2), 300 mM NaCl, 5 mM 2-mercaptoethanol, and 20% glycerol (v/v)). The protein-bound slurry was packed in a 2 ml Biorad column and washed with 60 ml buffer B containing 0.1% DDM. Protein was eluted using 300 mM imidazole in buffer B at pH 7.2, then dialyzed against storage buffer (25 mM Tris-HCl (pH 7.2), 150 mM NaCl, 2 mM 2-mercaptoethanol, 5% glycerol, 0.1 % DDM) overnight at 4°C. Protein was stored at 4°C. The purity and integrity of recombinant proteins were checked by SDS-PAGE gel.

Inhibition Assays. The UppP activity of compound **16** was investigated utilizing previously described methods.[48] Putative inhibitors for UppP were diluted in DMSO to designated

concentrations. For UppP inhibition, inhibitors were incubated with 20 nM of UppP at room temperature for 15 min in assay buffer (50 mM HEPES (pH 8), 150 mM NaCl, 10 mM $MgCl_2$, and 0.02% DDM) before adding 50 μM FPP to start the reaction. Reaction mixtures were incubated at 37 °C for 30 minutes, then quenched by the addition of equal volume malachite-green reagent.[49] Phosphate release was measured at 620 nm and values obtained were used to yield a dose-response curve. Data for all inhibition assays were analyzed in GraphPad Prism. Curves to determine IC_{50} values were plotted in log2 and were fit using variable slopes vs. log(inhibitor) for enzyme inhibition. The results are presented as percent UppP inhibition, in presence of different concentrations of compound **16**, relative to the untreated samples. Error bars represent standard deviation values obtained from six measurements from three independent experiments.

Murine MRSA skin infection experiment. The skin infection was performed as previously described[50] with some modifications. Briefly, six to eight-week-old female BALB/c mice, weighing 20 gm on average, were divided into three groups (n = 5/group) and their backs were shaven using a hair clipper. On the day of the infection, the mice were anesthetized using 2,2,2-tribromoethanol (25 μg/mL) and injected subcutaneously with 100 μL containing 4 x 10^9 CFU of MRSA USA300, suspended in 0.5% hydroxypropyl methylcellulose (HPMC) in sterile pyrogen-free saline. The mice were then returned to their cages and given food and water ad libitum. Seventy-two hours post-infection (day 3), the infection site was treated with either i) petroleum jelly (PG), ii) petroleum jelly containing 2% compound **16**, or iii) commercially-available topical cream containing 2% fusidic acid. The treatment continued on days 4, 5, and 6 twice daily. On day 7, the mice were euthanized with an overdose of anesthesia. A skin patch equivalent to ~ 1.5 cm^2, surrounding the lesion site, was excised aseptically from the from each mouse as well as the spleens. The skin patch was shredded with a sterile surgical blade then homogenized in 1 mL

pyrogen-free saline. While the spleen was homogenized in only 0.5 mL pyrogen-free saline. The homogenates were then, serially diluted, and plated on mannitol salt agar (MSA) plates for colony counts. Statistical analysis was performed using GraphPad Prism (version 6.0) (GraphPad Software, Inc., USA), applying one-way ANOVA, followed by the Tukey post-hoc test for multiple comparisons.

In vivo Toxicity study. BALB/C mice were dosed with compound **16** or vehicle by oral gavage (p.o.) at 250 mg/kg. Prior to administration, all mice were fasted (with water) for 10-14 h. For body weight change, all mice were weighed before dosing (Day 1) and at days 4, 7, and 10. For liver toxicity study, blood samples were drawn from submandibular vein 24 hr after dosing and serum enzymatic levels of transaminases (ALT and AST) were estimated calorimetrically according to the method of Reitman and Frankel.[51]

Murine systemic infection model. The systemic infection model was performed as previously described.[52-53] Briefly, three groups (n=5/group) of female 6-8-week old C57BL/6 mice were injected retro-orbitally with 100 µl containing ~10^7 CFU *S. aureus* strain USA300 suspended in sterile normal saline. Two hours post-infection, each mice group received intraperitoneally 100 µl of either sterile pyrogen-free phosphate buffered saline (PBS), compound **16** (20 mg/kg), or vancomycin (VA) (50 mg/ml). The treatment was repeated again at 24, 48, and 72 hours post-infection. After additional 24 hours following the last treatment does administration (96 hours post-infection), the mice were euthanized with an overdose of anesthesia followed by cervical dislocation. Then they were dissected, and their kidneys were harvested and aseptically homogenized in sterile normal saline, then serially diluted, and plated on MSA plates for colony counts.

Ethical approval

Animal procedures were approved by the Research Ethics Committee of the Faculty of Pharmacy, Cairo University (approval No.1682 and 2701) following the Guide for the Care and Use of Laboratory Animals published by the Institute of Laboratory Animal Research (USA).

ASSOCIATED CONTENTS

Supporting information. The supporting information is available free of charge on the ACS publication website. ^{1}H and ^{13}C NMR spectra of all newly described compounds, details about the microbiological, biochemical assays and pharmacokinetics.

Conflicts of interest

none to declare.

Abbreviations. CFU, colony forming unit; CL, clearance; int$T_{1/2}$, intrinsic half-life; MIC, minimum inhibitory concentration; MSSA, methicillin-sensitive *Staphylococcus aureus*; MRSA, methicillin-resistant *Staphylococcus aureus*; VRSA, vancomycin-resistant *Staphylococcus aureus*; VRE, vancomycin-resistance enterococci; UppP, undecaprenyl diphosphate phosphatase

.

Author information.

[I]These two authors contributed equally

ORCID

Nader S. Abutaleb: 0000-0003-1730-4150

Abdelrahman S. Mayhoub: 0000-0002-3987-3680

Acknowledgments. This work was funded by the Academy of Scientific Research and Technology, JESOUR-D program (Cycle 11; Project ID: 3092). The authors would like to thank ATCC and BEI Resources for providing the clinical isolates used in this study.

References

1. Tacconelli, E.; Magrini, N.; Kahlmeter, G.; Singh, N., Global priority list of antibiotic-resistant bacteria to guide research, discovery, and development of new antibiotics. World Health Organization **2017**, 27.

2. Centers for Disease Control and Prevention, "Deadly Staph Infections Still Threaten the U.S." March 5, 2019; accessed Jan. 13, 2020, https://www.cdc.gov/media/releases/2019/p0305-deadly-staph-infections.html#:~:text=More%20than%20119%2C000%20people%20suffered,Control%20and%20Prevention%20(CDC).

3. Rasmussen, R. V.; Fowler, V. G., Jr.; Skov, R.; Bruun, N. E., Future challenges and treatment of Staphylococcus aureus bacteremia with emphasis on MRSA. *Future Microbiol* **2011,** *6*, 43-56. DOI: 10.2217/fmb.10.155.

4. Im, J. H.; Baek, J. H.; Kwon, H. Y.; Lee, J. S., Incidence and risk factors of linezolid-induced lactic acidosis. *Int J Infect Dis* **2015,** *31*, 47-52. DOI: 10.1016/j.ijid.2014.12.009.

5. Abou Hassan, O. K.; Karnib, M.; El-Khoury, R.; Nemer, G.; Ahdab-Barmada, M.; BouKhalil, P., Linezolid Toxicity and Mitochondrial Susceptibility: A Novel Neurological Complication in a Lebanese Patient. *Front Pharmacol* **2016,** *7*, 325. DOI: 10.3389/fphar.2016.00325.

6. Azhar, A.; Rasool, S.; Haque, A.; Shan, S.; Saeed, M.; Ehsan, B.; Haque, A., Detection of high levels of resistance to linezolid and vancomycin in Staphylococcus aureus. *J Med Microbiol* **2017,** *66*, 1328-1331. DOI: 10.1099/jmm.0.000566.

7. Roch, M.; Gagetti, P.; Davis, J.; Ceriana, P.; Errecalde, L.; Corso, A.; Rosato, A. E., Daptomycin Resistance in Clinical MRSA Strains Is Associated with a High Biological Fitness Cost. *Front Microbiol* **2017,** *8*, 2303. DOI: 10.3389/fmicb.2017.02303.

8. Kirby, W. M., Extraction of a Highly Potent Penicillin Inactivator from Penicillin Resistant Staphylococci. *Science* **1944,** *99*, 452-453. DOI: 10.1126/science.99.2579.452.

9. Lasa, I., Towards the identification of the common features of bacterial biofilm development. *Int Microbiol* **2006,** *9*, 21-28.

10. Joller, N.; Weber, S. S.; Müller, A. J.; Spörri, R.; Selchow, P.; Sander, P.; Hilbi, H.; Oxenius, A., Antibodies protect against intracellular bacteria by Fc receptor-mediated lysosomal targeting. *Proceedings of the National Academy of Sciences* **2010,** *107*, 20441-20446.

11. Christmas, B. A. F.; Rolfe, M. D.; Rose, M.; Green, J., Staphylococcus aureus adaptation to aerobic low-redox-potential environments: implications for an intracellular lifestyle. *Microbiology* **2019,** *165*, 779-791. DOI: 10.1099/mic.0.000809.

12. von Eiff, C.; Peters, G.; Becker, K., The small colony variant (SCV) concept—the role of staphylococcal SCVs in persistent infections. *Injury* **2006,** *37*, S26-S33.

13. Moise-Broder, P. A.; Forrest, A.; Birmingham, M. C.; Schentag, J. J., Pharmacodynamics of vancomycin and other antimicrobials in patients with Staphylococcus aureus lower respiratory tract infections. *Clin Pharmacokinet* **2004,** *43*, 925-942. DOI: 10.2165/00003088-200443130-00005.

14. Eid, I.; Elsebaei, M. M.; Mohammad, H.; Hagras, M.; Peters, C. E.; Hegazy, Y. A.; Cooper, B.; Pogliano, J.; Pogliano, K.; Abulkhair, H. S.; Seleem, M. N.; Mayhoub, A. S., Arylthiazole antibiotics targeting intracellular methicillin-resistant Staphylococcus aureus (MRSA) that interfere with bacterial cell wall synthesis. *Eur J Med Chem* **2017,** *139*, 665-673. DOI: 10.1016/j.ejmech.2017.08.039.

15. ElAwamy, M.; Mohammad, H.; Hussien, A.; Abutaleb, N. S.; Hagras, M.; Serya, R. A. T.; Taher, A. T.; Abouzid, K. A.; Seleem, M. N.; Mayhoub, A. S., Alkoxyphenylthiazoles with broad-spectrum activity against multidrug-resistant gram-positive bacterial pathogens. *Eur J Med Chem* **2018,** *152*, 318-328. DOI: 10.1016/j.ejmech.2018.04.049.

16. Elsebaei, M. M.; Abutaleb, N. S.; Mahgoub, A. A.; Li, D.; Hagras, M.; Mohammad, H.; Seleem, M. N.; Mayhoub, A. S., Phenylthiazoles with nitrogenous side chain: An approach to overcome molecular obesity. *Eur J Med Chem* **2019,** *182*, 111593. DOI: 10.1016/j.ejmech.2019.111593.

17. Elsebaei, M. M.; Mohammad, H.; Abouf, M.; Abutaleb, N. S.; Hegazy, Y. A.; Ghiaty, A.; Chen, L.; Zhang, J.; Malwal, S. R.; Oldfield, E.; Seleem, M. N.; Mayhoub, A. S., Alkynyl-containing phenylthiazoles: Systemically active antibacterial agents effective against methicillin-resistant Staphylococcus aureus (MRSA). *Eur J Med Chem* **2018,** *148*, 195-209. DOI: 10.1016/j.ejmech.2018.02.031.

18. Hagras, M.; Abutaleb, N. S.; Ali, A. O.; Abdel-Aleem, J. A.; Elsebaei, M. M.; Seleem, M. N.; Mayhoub, A. S., Naphthylthiazoles: Targeting Multidrug-Resistant and Intracellular Staphylococcus aureus with Biofilm Disruption Activity. *ACS Infect Dis* **2018,** *4*, 1679-1691. DOI: 10.1021/acsinfecdis.8b00172.

19. Hagras, M.; Hegazy, Y. A.; Elkabbany, A. H.; Mohammad, H.; Ghiaty, A.; Abdelghany, T. M.; Seleem, M. N.; Mayhoub, A. S., Biphenylthiazole antibiotics with an oxadiazole linker: An approach to improve physicochemical properties and oral bioavailability. *Eur J Med Chem* **2018,** *143*, 1448-1456. DOI: 10.1016/j.ejmech.2017.10.048.

20. Hosny, Y.; Abutaleb, N. S.; Omara, M.; Alhashimi, M.; Elsebaei, M. M.; Elzahabi, H. S.; Seleem, M. N.; Mayhoub, A. S., Modifying the lipophilic part of phenylthiazole antibiotics to control their drug-likeness. *Eur J Med Chem* **2020,** *185*, 111830. DOI: 10.1016/j.ejmech.2019.111830.

21. Kotb, A.; Abutaleb, N. S.; Hagras, M.; Bayoumi, A.; Moustafa, M. M.; Ghiaty, A.; Seleem, M. N.; Mayhoub, A. S., tert-Butylphenylthiazoles with an oxadiazole linker: a novel orally bioavailable class of antibiotics exhibiting antibiofilm activity. *RSC Advances* **2019,** *9*, 6770-6778.

22. Kotb, A.; Abutaleb, N. S.; Seleem, M. A.; Hagras, M.; Mohammad, H.; Bayoumi, A.; Ghiaty, A.; Seleem, M. N.; Mayhoub, A. S., Phenylthiazoles with tert-Butyl side chain: Metabolically stable with anti-biofilm activity. *Eur J Med Chem* **2018,** *151*, 110-120. DOI: 10.1016/j.ejmech.2018.03.044.

23. Mancy, A.; Abutaleb, N. S.; Elsebaei, M. M.; Saad, A. Y.; Kotb, A.; Ali, A. O.; Abdel-Aleem, J. A.; Mohammad, H.; Seleem, M. N.; Mayhoub, A. S., Balancing Physicochemical Properties of Phenylthiazole Compounds with Antibacterial Potency by Modifying the Lipophilic Side Chain. *ACS Infect Dis* **2020,** *6*, 80-90. DOI: 10.1021/acsinfecdis.9b00211.

24. Mayhoub, A. S.; Marler, L.; Kondratyuk, T. P.; Park, E. J.; Pezzuto, J. M.; Cushman, M., Optimization of thiazole analogues of resveratrol for induction of NAD(P)H:quinone reductase 1 (QR1). *Bioorg Med Chem* **2012,** *20*, 7030-7039. DOI: 10.1016/j.bmc.2012.10.006.

25. Mohammad, H.; Reddy, P. V.; Monteleone, D.; Mayhoub, A. S.; Cushman, M.; Hammac, G. K.; Seleem, M. N., Antibacterial Characterization of Novel Synthetic Thiazole Compounds against Methicillin-Resistant Staphylococcus pseudintermedius. *PLoS One* **2015,** *10*, e0130385. DOI: 10.1371/journal.pone.0130385.

26. Mohammad, H.; Younis, W.; Chen, L.; Peters, C. E.; Pogliano, J.; Pogliano, K.; Cooper, B.; Zhang, J.; Mayhoub, A.; Oldfield, E.; Cushman, M.; Seleem, M. N., Phenylthiazole Antibacterial Agents Targeting Cell Wall Synthesis Exhibit Potent Activity in Vitro and in Vivo against Vancomycin-Resistant Enterococci. *J Med Chem* **2017,** *60*, 2425-2438. DOI: 10.1021/acs.jmedchem.6b01780.

27. Hagras, M.; Mohammad, H.; Mandour, M. S.; Hegazy, Y. A.; Ghiaty, A.; Seleem, M. N.; Mayhoub, A. S., Investigating the Antibacterial Activity of Biphenylthiazoles against Methicillin- and Vancomycin-Resistant Staphylococcus aureus (MRSA and VRSA). *J Med Chem* **2017,** *60*, 4074-4085. DOI: 10.1021/acs.jmedchem.7b00392.

28. Seleem, M. A.; Disouky, A. M.; Mohammad, H.; Abdelghany, T. M.; Mancy, A. S.; Bayoumi, S. A.; Elshafeey, A.; El-Morsy, A.; Seleem, M. N.; Mayhoub, A. S., Second-Generation Phenylthiazole Antibiotics with Enhanced Pharmacokinetic Properties. *J Med Chem* **2016,** *59*, 4900-4912. DOI: 10.1021/acs.jmedchem.6b00233.

29. Hussain, S. M.; Frazier, J. M., Cellular toxicity of hydrazine in primary rat hepatocytes. *Toxicol Sci* **2002,** *69*, 424-432. DOI: 10.1093/toxsci/69.2.424.

30. Antosiewicz, J.; Matuszkiewicz, A.; Olek, R. A.; Kaczor, J. J.; Ziolkowski, W.; Wakabayashi, T.; Popinigis, J., Content and redistribution of vitamin E in tissues of Wistar rats under oxidative stress induced by hydrazine. *Arch Environ Contam Toxicol* **2002,** *42*, 363-368. DOI: 10.1007/s00244-001-0033-2.

31. Tafazoli, S.; Mashregi, M.; O'Brien, P. J., Role of hydrazine in isoniazid-induced hepatotoxicity in a hepatocyte inflammation model. *Toxicol Appl Pharmacol* **2008,** *229*, 94-101. DOI: 10.1016/j.taap.2008.01.002.

32. Tomasi, A.; Albano, E.; Botti, B.; Vannini, V., Detection of free radical intermediates in the oxidative metabolism of carcinogenic hydrazine derivatives. *Toxicol Pathol* **1987,** *15*, 178-183. DOI: 10.1177/019262338701500208.

33. Costerton, J. W.; Stewart, P. S.; Greenberg, E. P., Bacterial biofilms: a common cause of persistent infections. *science* **1999,** *284*, 1318-1322.

34. Otto, M., Staphylococcus epidermidis—the'accidental'pathogen. *Nature reviews microbiology* **2009,** *7*, 555.

35. Khan, H. A.; Ahmad, A.; Mehboob, R., Nosocomial infections and their control strategies. *Asian pacific journal of tropical biomedicine* **2015,** *5*, 509-514.

36. CDC. Antibiotic Resistance Threats in the United States, 2019. Atlanta, GA: U.S. Department of Health and Human Services, CDC; 2019.

37. Cantoni, L.; Glauser, M. P.; Bille, J., Comparative efficacy of daptomycin, vancomycin, and cloxacillin for the treatment of Staphylococcus aureus endocarditis in rats and role of test conditions in this determination. *Antimicrob Agents Chemother* **1990,** *34*, 2348-2353.

38. Singh, S. R.; Bacon, A. E., 3rd; Young, D. C.; Couch, K. A., In vitro 24-hour time-kill studies of vancomycin and linezolid in combination versus methicillin-resistant Staphylococcus aureus. *Antimicrob Agents Chemother* **2009,** *53*, 4495-4497. DOI: 10.1128/AAC.00237-09.

39. Levine, D. P.; Fromm, B. S.; Reddy, B. R., Slow response to vancomycin or vancomycin plus rifampin in methicillin-resistant Staphylococcus aureus endocarditis. *Ann. Intern. Med.* **1991,** *115*, 674-680.

40. Vergidis, P.; Rouse, M. S.; Euba, G.; Karau, M. J.; Schmidt, S. M.; Mandrekar, J. N.; Steckelberg, J. M.; Patel, R., Treatment with linezolid or vancomycin in combination with rifampin is effective in an animal model of methicillin-resistant Staphylococcus aureus foreign body osteomyelitis. *Antimicrob Agents Chemother* **2011,** *55*, 1182-1186. DOI: 10.1128/AAC.00740-10.

41. Alder, J.; Eisenstein, B., The Advantage of Bactericidal Drugs in the Treatment of Infection. *Curr Infect Dis Rep* **2004,** *6*, 251-253. DOI: 10.1007/s11908-004-0042-1.

42. Gottlieb, H. E.; Kotlyar, V.; Nudelman, A., NMR chemical shifts of common laboratory solvents as trace impurities. *J. Org. Chem.* **1997,** *62*, 7512–7515.

43. CLSI, *Methods for Dilution Antimicrobial Susceptibility Tests for Bacteria That Grow Aerobically; Approved Standard*. January 2012; Vol. Ninth Edition M07-A9. 32 No. 2.

44. Hammad, A.; Abutaleb, N. S.; Elsebaei, M. M.; Norvil, A. B.; Alswah, M.; Ali, A. O.; Abdel-Aleem, J. A.; Alattar, A.; Bayoumi, S. A.; Gowher, H.; Seleem, M. N.; Mayhoub, A. S., From Phenylthiazoles to Phenylpyrazoles: Broadening the Antibacterial Spectrum toward Carbapenem-Resistant Bacteria. *J Med Chem* **2019,** *62*, 7998-8010. DOI: 10.1021/acs.jmedchem.9b00720.

45. Opoku-Temeng, C.; Naclerio, G. A.; Mohammad, H.; Dayal, N.; Abutaleb, N. S.; Seleem, M. N.; Sintim, H. O., N-(1,3,4-oxadiazol-2-yl)benzamide analogs, bacteriostatic agents against methicillin- and vancomycin-resistant bacteria. *European Journal of Medicinal Chemistry* **2018,** *155*, 797-805. DOI: 10.1016/j.ejmech.2018.06.023.

46. Garcia, L. S., Clinical microbiology procedures handbook. American Society for Microbiology Press (ASM press), Washington DC: 2010; Vol. 1.

47. Eissa, I. H.; Mohammad, H.; Qassem, O. A.; Younis, W.; Abdelghany, T. M.; Elshafeey, A.; Abd Rabo Moustafa, M. M.; Seleem, M. N.; Mayhoub, A. S., Diphenylurea derivatives for combating methicillin- and vancomycin-resistant Staphylococcus aureus. *Eur J Med Chem* **2017,** *130*, 73-85. DOI: 10.1016/j.ejmech.2017.02.044.

48. Elsebaei, M. M.; Mohammad, H.; Samir, A.; Abutaleb, N. S.; Norvil, A. B.; Michie, A. R.; Moustafa, M. M.; Samy, H.; Gowher, H.; Seleem, M. N.; Mayhoub, A. S., Lipophilic efficient phenylthiazoles with potent undecaprenyl pyrophosphatase inhibitory activity. *Eur J Med Chem* **2019,** *175*, 49-62. DOI: 10.1016/j.ejmech.2019.04.063.

49. Desai, J.; Wang, Y. D.; Wang, K. D.; Malwal, S. R. D.; Oldfield, E., Isoprenoid Biosynthesis Inhibitors Targeting Bacterial Cell Growth. *ChemMedChem* **2016,** *11*, 2205-2215. DOI: 10.1002/cmdc.201600343.

50. Tseng, C. W.; Sanchez-Martinez, M.; Arruda, A.; Liu, G. Y., Subcutaneous infection of methicillin resistant Staphylococcus aureus (MRSA). *J Vis Exp* **2011**. DOI: 10.3791/2528.

51. Reitman, S.; Frankel, S., A colorimetric method for the determination of serum glutamic oxalacetic and glutamic pyruvic transaminases. *Am J Clin Pathol* **1957,** *28*, 56-63. DOI: 10.1093/ajcp/28.1.56.

52. Attia, A. S.; Schroeder, K. A.; Seeley, E. H.; Wilson, K. J.; Hammer, N. D.; Colvin, D. C.; Manier, M. L.; Nicklay, J. J.; Rose, K. L.; Gore, J. C.; Caprioli, R. M.; Skaar, E. P., Monitoring the inflammatory response to infection through the integration of MALDI IMS and MRI. *Cell host & microbe* **2012,** *11* (6), 664-73. DOI: 10.1016/j.chom.2012.04.018.

53. Attia, A. S.; Cassat, J. E.; Aranmolate, S. O.; Zimmerman, L. J.; Boyd, K. L.; Skaar, E. P., Analysis of the *Staphylococcus aureus* abscess proteome identifies antimicrobial host

proteins and bacterial stress responses at the host-pathogen interface. *Pathog Dis* **2013,** *69*, 36-48. DOI: 10.1111/2049-632X.12063.

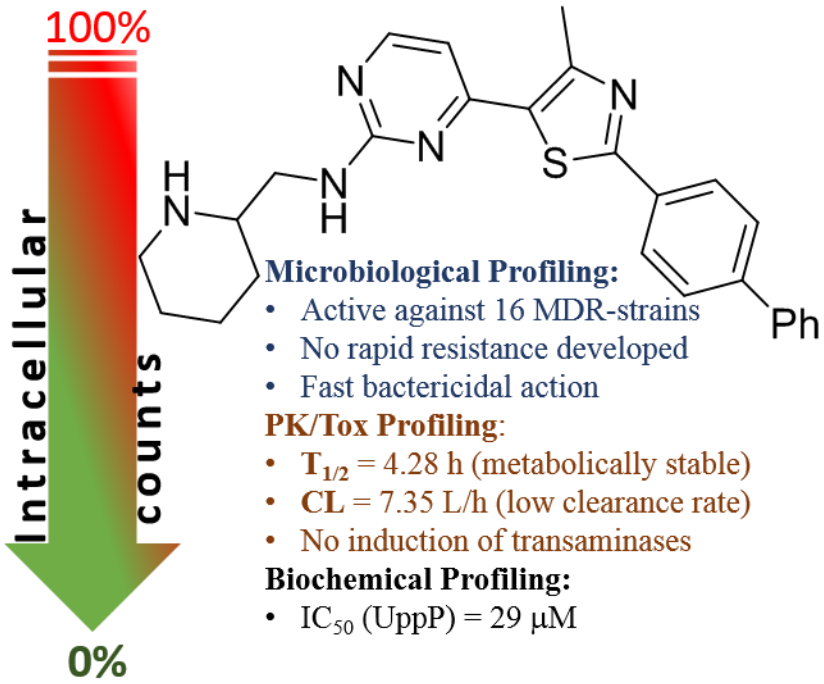

Microbiological Profiling:

- Active against 16 MDR-strains
- No rapid resistance developed
- Fast bactericidal action

PK/Tox Profiling:

- $T_{1/2}$ = 4.28 h (metabolically stable)
- **CL** = 7.35 L/h (low clearance rate)
- No induction of transaminases

Biochemical Profiling:

- IC_{50} (UppP) = 29 μM